Inter-annual and seasonal trends of vegetation condition in the Upper Blue Nile (Abay) basin: Dual scale time series analysis

E. Teferi [1*], S. Uhlenbrook[2,3], W. Bewket [4]

[1] *Addis Ababa University, Center for Environment and Development Studies, P.O. Box 2176, Addis Ababa, Ethiopia*
[2] *UNESCO-IHE Institute for Water Education, P.O. Box 3015, 2601 DA Delft, The Netherlands*
[3] *Delft University of Technology, Water Resources Section, P.O. Box 5048, GA Delft, The Netherlands*
[4] *Addis Ababa University, Department of Geography and Environmental Studies, P.O. Box 2176, Addis Ababa, Ethiopia*

Abstract

A long-term decline in ecosystem functioning and productivity, often called land degradation, is a serious environmental and development challenge to Ethiopia that needs to be understood so as to develop sustainable land use strategies. This study examines inter-annual and seasonal trends of vegetation cover in the Upper Blue Nile (UBN) or Abbay basin. Advanced Very High Resolution Radiometer (AVHRR) based Global Inventory, Monitoring, and Modelling Studies (GIMMS) Normalized Difference Vegetation Index (NDVI) was used for long-term vegetation trend analysis at low spatial resolution. Moderate-resolution Imaging Spectroradiometer (MODIS) NDVI data (MOD13Q1) was used for medium scale vegetation trend analysis. Harmonic analyses and non-parametric trend tests were applied to both GIMMS NDVI (1981–2006) and MODIS NDVI (2001-2011) data sets. Based on a robust trend estimator (Theil-Sen slope) most part of the UBN (~77%) showed a positive trend in monthly GIMMS NDVI with a mean rate of 0.0015 NDVI units (3.77% yr^{-1}), out of which 41.15% of the basin depicted significant increases ($p < 0.05$) with a mean rate of 0.0023 NDVI units (5.59% yr^{-1}) during the period. However, the MODIS-based vegetation trend analysis revealed that about 36% of the UBN shows a significantly decreasing trend ($p < 0.05$) over the period 2001-2011 at an average rate of 0.0768 NDVI yr^{-1}. This indicates that the greening trend of vegetation condition was followed by browning trend since the mid-2000s in the basin, which requires the attention of land users and decision makers. Seasonal trend analysis was found to be very useful in identifying changes in vegetation condition that could be masked if only inter-annual vegetation trend analysis was performed. Over half (60%) of the Abay basin were found to exhibit significant trends in seasonality over the 25 years period (1982-2006). About 17% and 16% of the significant trends consisted of areas experiencing a uniform increase in NDVI throughout the year and extended growing season, respectively. These areas were found primarily in shrubland and woodland regions. The MODIS-based trend analysis revealed trends that were mainly linked to human activities. This study concludes that integrated analysis of inter-annual and intra-annual

---

* Correspondence to: ermias52003@yahoo.com

trends based on GIMMS and MODIS enables a more robust identification of changes in vegetation condition.

Key words: Upper Blue Nile/Abay; inter-annual; intra-annual; trend analysis; AVHRR; MODIS

Introduction

Land degradation is a widespread environmental and development challenge (e.g.Dregne et al., 1991; UNEP, 2007). It is central to many international conventions and protocols related to environmental protection. Increasing demands for food, water and energy resulting from the growth in population and *per capita* consumption are driving unprecedented land use change (Godfray et al., 2010; Kearney, 2010). In turn, unsustainable land use is causing degradation of land resources. Thus, up-to-date quantitative information about land degradation is crucial to develop sustainable land use strategies and to support policy development for food and water security and environmental integrity. Status and trend of vegetation condition generally serve as a proxy for land degradation (Metternicht et al., 2010; Wessels et al., 2004; Wessels et al., 2007).

Detecting and characterizing trends in vegetation condition over time using remotely sensed data has received considerable attention in recent years (Bai et al., 2008; de Jong et al., 2011; Eastman et al., 2013; Verbesselt et al., 2010a). Recent interest in vegetation trend analysis arises for three reasons. First, there is considerable interest in monitoring and assessing the state and trend of land degradation as well as for monitoring the performance of management programs (Buenemann et al., 2011; Vogt et al., 2011). Second, it is only recently that substantial amounts of remotely sensed data and robust geospatial approaches suitable to such analysis are becoming available (Bai et al., 2008; Buenemann et al., 2011; Tucker et al., 2005). Third, it is a natural first step toward identifying drivers of changes in terrestrial ecosystems as vegetation variability and trends affect the exchange of water, energy, nutrients and carbon between the biosphere, the geosphere and the atmosphere (Baldocchi et al., 2001).

Changes in vegetation occur in three ways: (1) a seasonal or cyclic change that is driven by climate (e.g. annual temperature and rainfall) impacting plant phenology; (2) a gradual change over time that is consistent in direction (monotonic) such as change in land management or land degradation; and (3) an abrupt shift at a specific point in time (step trend) that may be caused by disturbances such as a sudden change in land use policies, deforestation, floods, droughts, and

fires (Angert et al., 2005; de Jong et al., 2013a; Slayback et al., 2003; Tucker et al., 2001; Verbesselt et al., 2010b). Thus, considering all types of changes (i.e. seasonal, gradual and abrupt changes) is essential in order to assess the environmental impact of vegetation changes or to be able to attribute the changes in vegetation to drivers behind (de Jong et al., 2013a; Verbesselt et al., 2010b). There is substantial interest in monitoring the trends in seasonality of vegetation due to its sensitive response to climate change (Parmesan and Yohe, 2003; Sparks et al., 2009; Walther et al., 2002).

Long-term, remotely sensed normalized difference vegetation index (NDVI) data are suitable to detect and characterize trends in vegetation condition over time (de Jong et al., 2011; Eastman et al., 2013; Tucker et al., 2001; Verbesselt et al., 2010a). Although NDVI can be computed from different multispectral satellite data, NDVI from Advanced Very High Resolution Radiometer (AVHRR) is the only global vegetation dataset which spans a time period of three decades. Hence, it allows quantification of ecosystem changes as a result of ecosystem dynamics and varying climate conditions. In this study, AVHRR based Global Inventory, Monitoring, and Modelling Studies (GIMMS) NDVI data sets (1981–2006) were used for the purpose of long-term trend analysis (Tucker et al., 2005). Besides, NDVI time series (2001-2011) from the Moderate resolution Imaging Spectroradiometer (MODIS) 250m (MOD13Q1) on board the Earth Observing System Terra platform were used for medium scale vegetation trend analysis.

Several vegetation trend studies from analysis of satellite observations have reported increasing trend of greenness in the Northern Hemisphere, including the Sahel (Fensholt et al., 2009; Karlsen et al., 2007; Slayback et al., 2003; Tucker et al., 2001). Other studies based on phenology and temperature observations from stations also confirmed greenness trends (Sparks et al., 2009). However, Zhao and Running (2010) reported a decreasing trend in greenness globally during the period 2000-2009 using Moderate-resolution Imaging Spectroradiometer (MODIS) NDVI data. Similarly, de Jong et al. (2011) found that many forested biomes experienced a decline in vegetation greenness. There is still no consistent result on trends of global vegetation activity (Bala et al., 2013).

The inconsistent results from various studies potentially emanated from differences in location of study areas (variations in altitude and latitude), trend detection techniques (ordinary least square versus median trend), the length of the data series and NDVI data sources used (e.g. GIMMS, MODIS). Therefore, it is very important to characterize and understand inter-annual and intra-annual variability of vegetation activity using long-term data sets in study areas such as Abbay basin (1982-2006) where climate variability is high and topography is diverse.

It is essential to characterize and understand inter-annual and intra-annual variability of vegetation activity using long-term data sets such as GIMMS NDVI, especially, if the increase or decrease of vegetation growth in Abay basin is mainly driven by climatic factors (De Beurs et al., 2009). However, if vegetation growth is mainly caused by human activities such as sustainable land management (SLM) programs that involve localized implementation of best management practices (BMPs), then it is useful to use MODIS NDVI data as it provides repeated information at the spatial scale at which most human-driven land cover changes occur (De Beurs et al., 2009; Gallo et al., 2005; Townshend and Justice, 1988). Such analysis reveals areas of change that merit closer attention since it depicts significant shifts in local water, carbon and energy fluxes (Henebry, 2009; Vuichard et al., 2008). The results of this study are very important from context of Upper Blue Nile (UBN) basin for two reasons. First, the UBN basin is the major water source area of the Nile river, as it contributes around 70% of the overall Nile flow. Thus, the UBN basin is the most important river basin not only for Ethiopia, but also for the downstream Nile basin countries (i.e. Sudan and Egypt). Second, the UBN basin accounts for a major share of the Ethiopia's irrigation and hydropower potential.

The general objective of this study was to characterize the degree of improvement or degradation of vegetation condition in the Abay basin using both coarse and medium scale analysis. The specific objectives were: (1) to identify inter-annual and seasonal trends in vegetation conditions at both coarse and medium scales using robust trend estimators; and (2) to detect trend breaks.

2. Materials and methods

2.1 Study area

The Upper Blue Nile/Abbay basin covers a total area of 199,812 km^2 and is located in the center and west of Ethiopia (Fig. 1). It lies approximately between 7°45' and 12°46' N, and 34°06' and 40°00' E. Altitude of the Upper Blue Nile basin ranges from 475 m asl at the Sudanese border to 4,257 m asl at the summit of Mt. Guna. More than 83% of the basin is located at an elevation above 1,000 m asl. The multi-year (1983-2006) mean annual rainfall varies between about 894 mm a-1 to 1,909 mm a-1, with a spatial mean of about 1,396 mm a-1 based on gridded station-based rainfall data. The multi-year (1982-2006) mean annual areal potential evaporation ranges from 1065 mm a-1 to 1756 mm a-1, with a spatial mean of about 1,396 mm a-1 based on the Penman–Monteith method from Climate Research Unit 3.10 data set (Harris et al., 2014). The multi-year (1982-2006) annual average temperature varies across space from 14°C to 29°C based on CRU 3.10 data set.

Cropland is the major land use and land cover type, occupying more than 44% of the total area of the basin (TECSULT, 2004). A variety of annual crops are grown under rainfed conditions including: wheat, barley, sorghum, *teff*, maize, finger millet, oil seeds, chick peas and beans. *Eucalyptus* plantation mainly for wood and fuel wood is common in areas near villages. Extensive areas of *bamboo* occur in the lower areas of the western part of the basin. Dense woodland is mainly found on the lower western slopes in *Wellega*, *North Gondar* and *Benishangul-Gumuz*; open woodland is found notably in Wellega, Illubabor and Jimma; and open shrubland in highland areas. Woodlands and shrublands are often associated with a grass under-storey or grassed areas between areas of low woody vegetation. Two main types of grassland occur in the basin; (a) *Lowland tall grasslands* occur in low rainfall areas interspersed with a few trees and shrubs, and (b) *Highland temperate grasslands* occur mainly above 2,000 masl.

2.2 Data sets

GIMMS 15-day composite NDVI product: The Global Inventory, Monitoring, and Modelling Studies (GIMMS) NDVI data product (Tucker et al., 2005), was used to analyze the long-term

(1982-2006) vegetation variability and trends in UBN basin. A release of the global coverage GIMMS data (GIMMSg) at 8 km resolution, covering from July 1981 through December 2006, was made freely available from the Global Land Cover Facility of the University of Maryland (www.landcover.org). The GIMMSg data set is composited at a 15-day time step by applying maximum value compositing (MVC) technique (Holben, 1986) in order to reduce cloud cover and water vapor effects.

MODIS NDVI 16-Day L3 Global 250m (MOD13Q1): The MODIS 16-day composite NDVI data sets with 250 m spatial resolution (MOD13Q1) tiles of h21v07 and h21v08 for the period 2001–2011 obtained from the NASA Earth Observing System (EOS) data gateway were used in this study (Huete et al., 2002). The MODIS NDVI complements NOAA's AVHRR derived NDVI products and provides continuity for time series historical applications. Apart from the vegetation index, the MOD13Q1 data contains pixel reliability information describing overall quality of NDVI values for each pixel. Pixel reliability information is a simple decimal number that ranks the product into five categories: -1— Fill/No Data, 0—Good Data, 1—Marginal Data, 2—Snow/Ice, and 3—Cloudy. In the time series analysis, only 'good' = 0 data are retained and all other values are interpolated or replaced.

Land use and land cover (LULC) data: The third data set used in the analysis was *LULC* data produced by Woody Biomass Inventory and Strategic Planning Project (WBISPP) at a scale of 1:250,000 (TECSULT, 2004). The intention was to provide a basis for understanding the spatial distribution of seasonal trends.

2.3 Harmonic analysis of NDVI time-series

Both AVHRR and MODIS NDVIs are composite products. Since Maximum Value Composite (MVC) is not an atmospheric-correction method, some artefacts related to residual cloud cover and atmospheric haze remain in the MVC processed NDVI series (Nagol et al., 2009). Therefore, it was essential to perform harmonic analysis of both GIMMSg and MODIS NDVI data sets using HANTS (Harmonic ANalysis of Time Series) algorithm (Roerink et al., 2000; Verhoef et al., 1996) for the purpose of: (i) screening and removal of cloud contaminated observations; and (ii) temporal interpolation of the remaining observations to reconstruct gapless images at a prescribed time. Harmonic (Fourier) analysis has been successfully applied to describing

precipitation patterns (e.g.Landin and Bosart, 1989), meteorology (e.g.Legates and Willmott, 1990) and seasonal and interannual variations in land surface condition (Jakubauskas et al., 2001). The HANTS algorithm was developed based on the concept of Discrete Fourier Transform. HANTS considers only the most significant frequencies expected to be present in the time profiles, and applies a least squares curve fitting procedure based on harmonic components (sine and cosine). Thus, harmonic (Fourier) analysis decomposes a time-dependent periodic phenomenon (e.g. vegetation development) into a series of sinusoidal functions, each defined by unique amplitude (strength) and phase (orientation with respect to time) (Roerink et al., 2000; Verhoef et al., 1996) and can be described as the sum of sine and cosine components as follows (Harris and Stöcker, 1998; Wilks, 2011):

$$f(t) = \alpha_0 + \sum_{n=1}^{n=2} C_n \cos(\omega_n t - \varphi_n) \quad (1.a)$$

$$= \alpha_0 + \sum_{n=1}^{n=2} \left\{ a_n \sin\left(\frac{2\pi n t}{T}\right) + b_n \cos\left(\frac{2\pi n t}{T}\right) \right\} + e \quad (1.b)$$

where *f(t)* is the series value at time *t*, *T* is the length of the series (e.g. T=12 observations for a monthly time series), *n* is the number of harmonics to be used in the regression (in this study 2 harmonics were used), α_0 is the mean of the series, C_n is the amplitude of harmonics given by $C_n = \sqrt{a_n^2 + b_n^2}$, ω_n is the frequency (2πn/T), φ_n is the phase angle given by $\varphi_n = \tan^{-1}(b_n/a_n)$ and *e* is the error term. Eq. (1.a) emphasizes the harmonic interpretation, while Eq. (1.b) is a convenient transformation to a multiple linear harmonic regression model with coefficients $a_n = C_n \cos(\varphi_n)$ and $b_n = C_n \sin(\varphi_n)$ that can be easily estimated.

In this study the IDL implementation of the HANTS algorithm (De Wit and Su, 2005) was used. In HANTS algorithm a curve fitting is applied iteratively and the maximum iteration was set to 12 (Table 1). First a least squares curve is computed based on all data points, and next the observations are compared to the curve. Observations that are clearly below the curve are candidates for rejection due to atmospheric contamination, and the points that have the greatest negative deviation from the curve therefore are removed first. Next a new curve is computed based on the remaining points and the process is repeated. Pronounced negative outliers are removed by assigning a weight of zero to them, and a new curve is computed. This iteration eventually leads to a smooth curve that approaches the upper envelope over the data points.

Essential HANTS parameters were set as in Table 1 in order to obtain a reliable fitting curve. Detail explanation about the parameters can be found in Roerink et al. (2000). . Although he output comprises five Fourier components (i.e.3 amplitudes and 2 phases), the zero frequency (mean annual NDVI) and the frequencies with time periods of 1 year (annual) were selected for the analysis Amplitude 2 and Phase 2 represent the semi-annual curve, but they are difficult to interpret (Eastman et al., 2013). This suite of harmonics (Amplitude 0, Amplitude 1 and Phase 1) is sometimes called *greenness parameters*.

2.4. Long-term trend analysis

Before the time series analysis, the bimonthly HANTS filtered GIMMS and MODIS data were aggregated to monthly composites by applying the arithmetic mean of each month. The bi-monthly composites usually show strong serial autocorrelation and aggregating into monthly observations reduces the effect of serial autocorrelation on the statistics generated from them. Seasonal variation must be removed in order to better discern the long-term trend in NDVI over time. Thus, a seasonally adjusted series is needed in order to better discern any trend that might otherwise be masked by seasonal variation. Standardized anomalies (Z-score) of the monthly HANTS filtered NDVI data were calculated to remove the seasonality from the original time series (i.e. *de-seasoning*) using the following equation:

$$Z = (x - \mu)/\sigma \quad (2)$$

where x is the data value of the respective month, μ is the monthly long term average value (i.e., the long term average of all Januaries, Februaries, …) and σ is the monthly standard deviation. A Z-score value of 0 would mean that it has a value equal to the long-term mean; a value of +1 would mean that it is 1 standard deviation of the long term mean, and so on.

The de-seasoned monthly NDVI time-series was corrected for serial correlation (autocorrelation) using a Trend Preserving Prewhitening (TPP) approach (Wang and Swail, 2001). The prewhitened series has the same trend as the original series, but with no serial correlation. Two types of inter-annual trend analysis and one trend significance test were applied to pre-whitened data on a pixel basis: linear trend (median trend or Theil-Sen), monotonic trend (Mann-Kendall) and Mann-Kendall significance test.

The median trend (Theil-Sen (TS)) was computed for assessing the linear trend and rate of change per unit time (Hoaglin et al., 1983). Theil-Sen (TS) slope estimator was proposed by

Thiel (1950) and modified by Sen (1968) and computes the median of the slopes between observation values at all pair-wise time steps. The major advantage of TS slope estimator is because of its breakdown bound. The breakdown bound for a robust statistic is the number of wild values that can occur within a series before it will be affected. For the median trend, the breakdown bound is approximately 29%, meaning that the trends expressed in the image must have persisted for more than 29% of the length of the series (in time steps) (Hoaglin et al., 1983). For example, in this study the GIMMS time series data contains 300 monthly images so it is completely unaffected by wild and noisy values unless they persist for more than 87 months (i.e.0.29*300=7.25 years). The implication of this is that it also ignores the effects of short-term inter-annual climate teleconnections such as El Niño (typically a 12 months effect) and La Niña (typically a 12-24 months effect).

2.5 Seasonal trend analysis

Seasonal trend analysis was performed in order to identify trends in the essential character of the seasonal cycle while rejecting noise and short-term variability seasonal cycle (Eastman et al., 2013). This was performed based on a two-stage time series analysis. First, harmonic regression is applied to each year of images in the time series to extract an annual sequence of overall greenness and the amplitude and phase of annual and semi-annual cycles (Eastman et al., 2009). This suite of harmonics is termed as greenness parameters. Amplitude 0 represents the annual mean NDVI or overall greenness for each year. Amplitude 1 represents the peak of annual greenness. Phase 1 denotes the timing of annual peak greenness, represented by the position of the starting point of the representative sinewave of annual greenness. An increase or decrease in the phase angle means a shift in the timing to an earlier or later time of the year, respectively. The values of Phase image potentially ranges from 0 degree to 359 degrees such that each 30 degrees indicates a shift of approximately one calendar month (Eastman et al., 2009). Amplitude 2 and Phase 2 represent the magnitude and position of a semi-annual curve, but their interpretation is difficult. They exist mainly as shape modifier of the annual curve (Eastman et al., 2013).Second, trends over years in the greenness parameters were analyzed using a Theil-Sen median slope operator. This procedure is robust to short-term interannual variability up to a period of 29% of the length of the series (Eastman et al., 2013; Gilbert, 1987; Hoaglin et al., 1983). Furthermore, the samples are annual measures of shape parameters. Thus, short inter-

annual disturbances (*i.e.*, those 8 years or less in this case) such as individual El Niño/Southern Oscillation events, have little effect on the long-term trends represented by the median trends. The significance of the trends in the five shape parameters was tested using the Contextual Mann Kendall statistics (CMK) (Neeti and Eastman, 2011) which is a modified form of the Mann-Kendall test of trend significance (Kendall, 1948; Mann, 1945). CMK trend test reduces the detection of spurious trends and an amplification of confidence when consistent trends are present through adding contextual information. CMK is a modified version of the Mann-Kendall test which is based on a principle that a pixel would not be expected to exhibit a radically different trend from neighbouring pixels.

In order to make the interpretation easier, the seasonal trends were categorized into different classes based on major CMK trend significance. The CMK trend significance for each of the five shape parameters was classified into three major categories: significantly decreasing at the $p < 0.05$ level, not significant, and significantly increasing at the $p < 0.05$ level. Only the major seasonal trend classes in terms of area were selected for detailed analysis.

2.6 Change-point analysis

A change-point analysis was conducted, because it indicates that the trends change between positive and negative within the analysis period. Regions of interest (ROIs) were selected based on most prevalent classes of significant seasonal trends for GIMMS NDVI and MODIS NDVI. The Breaks For Additive Seasonal and Trend (BFAST) method (Verbesselt et al., 2010a; Verbesselt et al., 2010b) were used to detect and characterize abrupt changes within the trend and seasonal components of the ROI times series. BFAST is particularly important if long-term trends are composed of consecutive segments with gradual change, separated from each other by a relatively short period of abrupt change (de Jong et al., 2012; Verbesselt et al., 2010b). In BFAST, the ordinary least squares (OLS) residuals-based MOving SUM (MOSUM) test, is used to test for whether one or more breakpoints are occurring. Thus, the use of BFAST trend break analysis assisted identification of several change periods which might otherwise been overlooked through a commonly assumed fixed change trajectory analysis. BFAST is an iterative algorithm that integrates the decomposition of time series into seasonal, trend, and remainder component with methods for detecting changes. An additive decomposition model is used to iteratively fit a

piecewise linear trend and a seasonal model. The general model is of the form: $Y_t = T_t + S_t + e_t$, $(t \in m)$, where Y_t is the observed NDVI data at time t (in the time series m), T_t is the trend component, S_t is the seasonal component, and e_t is the remainder component. A trend component corresponds to a long-term process that operates over the time spanned by the series. A remainder component corresponds to a local process which causes variability between cycles. A seasonal component corresponds to a cyclic process that operates within each cycle.

3. Results

3.1. Inter-annual trends in NDVI

3.1.1 GIMMS NDVI

The Upper Blue Nile (Abay) basin is characterized by a multi-year mean NDVI of 0.49 for the period 1982–2006 using the GIMMS data set. On the one hand, the south and southwest region of the basin represents the highest mean NDVI and the lowest temporal variation. This area is characterized by shrubland and woodland vegetation. On the other hand, the eastern, northeastern and northwestern part represents the lowest mean NDVI and the highest temporal variation as a consequence of the relatively low annual precipitation and the more extended dry periods. Besides, this area is characterized by intensive and sedentary cultivation.

During the period 1982-2006, a significantly increasing trend in vegetation condition is observed in large part of the basin particularly in western and central part of the basin (Fig. 2). About 77% of the basin showed a positive trend in monthly NDVI with a mean rate of 0.018 NDVI yr^{-1} (i.e. 0.0015*12 NDVI units) and the remaining 23% of the basin exhibited a decreasing trend with a mean rate of 0.0084 NDVI yr^{-1} (i.e. 0.0007*12) (Table 2). The monthly NDVI increased significantly (p<0.05) over 41.15% of the basin area, with a mean rate of 0.03 NDVI yr^{-1} (0.0023*12) and decreased significantly over 4.6% of the basin, with a mean rate of 0.02 NDVI yr^{-1} (0.0017*12).

3.1.2 MODIS NDVI

Areas of higher multi-year mean NDVI depict lower vegetation cover variability (Fig.3(a) and Fig. 3(b)). Areas located in the eastern part of the basin are those with higher variability and show an upward (positive) trend of vegetation growth in the period 2001-2011 (Fig.3(b) and Fig.3(c)). About 36% of the UBN/Abay basin shows a significantly browning trend ($p < 0.05$) over the period 2001-2011 at an average rate of 0.0768 NDVI yr^{-1} using MODIS 250 m spatial resolution (Table 3 and Table 4). By contrast, only about 1.19% of the basin shows a significantly greening trend ($p < 0.05$) over the period 2001-2011 at an average rate of 0.066 NDVI yr^{-1} (Table 3 and Table 4). The majority of this browning trend comes from Dabus (14.27% at a rate of 0.0744), Belles (13.5% at a rate of 0.0816), Wonbera (11.81% at a rate of

0.0792) and Didessa (11.48% at a rate of 0.0792). The vegetation activity in Belles sub basin is being decreased at a faster rate (0.0816 NDVI yr^{-1}) than the others (Table 3 and Table 4).

The Maximum significant browning slope observed in Didessa sub-basin is the largest of all maximum slopes in the basin. The size of greening and the browning area within sub-basins are proportional in sub-basins such as Beshillo, Jemma, Muger and Welaka. Whereas, more than half of the areas of the Belles (66.91%), Rahad (60.41%), and Wonbera (64.12%) are represented by significant browning trend. The majority of this greening trend comes from Jemma (22.03% at a rate of 0.066), Beshillo (18.23% at a rate of 0.066), North Gojam (22.78% at a rate of 0.066), and Muger (12.15% at a rate of 0.0648) sub-basins. The slowest rate and the fastest rate of significant greening are observed in Dinder sub-basin (0.0552 NDVI yr^{-1}) and Dabus sub-basin (0.0768 NDVI yr^{-1}), respectively.

3.2 Seasonal trends

3.2.1 GIMMS NDVI

More than half (59.52%) of land areas exhibit a significant trend in seasonality over the 25 year time period measured (1982-2006), producing a total of 53 significantly trending classes of seasonal curves which include different combinations of significant changes in Amplitude 0, Amplitude 1, Amplitude 2, Phase 1 and Phase 2. Thus, a trend change in seasonality is not a rare occurrence in Abay basin. Out of the 53 classes, only the prominent five classes of seasonal trends are described below, which account for about 67% of all significantly trending pixels and represent 39.95% of all land pixels of the basin. Figure 4 depicts the spatial distribution of the five most prevalent classes of significant seasonal trends in GIMMS NDVI.

Class 1 has an area of 19,712 km^2 which accounts for 16.85% of all significantly trending areas and 10.03% of the total land area (Table 5). This class represents areas with a significantly positive trend in Amplitude 0 (mean annual NDVI) and no significant change in any of the other four parameters (Amplitudes, Phases 1 and Phase 2), producing curves that are raised uniformly throughout the year. The frequency distribution of seasonal trend classes within zones of land cover types shows that the majority of Class 1 trending pixels occur in areas of woodland (33%) and shrubland (30%). Thus, it appears that woodland and shrubland areas are experiencing a consistent increase in productivity throughout the year.

Class 2 is characterized by both a significant increase in Amplitude 0 (mean annual NDVI) and a significant decrease in Phase 1 (orientation with time of the annual cycle). A decreasing phase angle means a shift to a later time of the year. This class has an area of 18,560 km^2 and describes about 10% of the basin land area (Table 5). Figure 5(b) shows that the green-down period is coming about 15 days later in 2006 than 1982. About 56% of Class 1 trending pixels occur in areas of woodland. This means that woodland areas of the Upper Blue Nile/Abay basin are experiencing an increase in mean annual NDVI with significant shift in end of growing season and no effect on the start of growing season leading to lengthening of the growing season.

Class 3 represents areas that exhibit a significant increase in Amplitude 1 (the annual cycle), but no other significant trend parameters. Class 3 covers 3.48% (6848 km^2) of all the basin area (Table 5). This class of seasonal trend exhibits a characteristic of increase in NDVI during the growing season (Aug-Nov) balanced by declines during the dry season (Feb-May) in order to maintain the same mean NDVI (Fig.5(c)). The majority of Class 3 trending pixels occur in cropland areas (68% or 4,672 km^2) of the basin. Therefore, NDVI is enhanced during the green season (cropping season) and inhibited during the brown season or harvest.

Class 4 represents areas that exhibit a significant decrease in Amplitude 1 (the annual cycle), but no other significant trend parameters. Class 4 covers 9.51% (18,688 km^2) of all the basin area (Table 5). This class of seasonal trend exhibits a characteristic decrease in NDVI during the growing season (more pronounced between Aug-Nov) increase in NDVI during dry season (Fig. 5(d)). Class 4 seasonal trend pixels are mostly associated with cropland (59%) and grassland (19%) land cover types. This type of seasonal trend is more common in North Gojam and Lake Tana sub-basins.

Class 5 describes areas that show a significant decrease in Phase 1 only. Class 5 seasonal curves resemble Class 2 seasonal curves in that both have similar pattern of a decrease in yearly phase. It covers 7.5% (14 720 km^2) of all the basin area and represents 12.6% of all significant seasonal trend pixels. This class of seasonal trend exhibits a characteristic shift in the end of growing season. Class 5 pixels are mostly associated with woodland (48%) and cropland (30%). This type of seasonal trend is more common in southern and southwestern part of the basin.

3.2.2 MODIS NDVI

About 207 classes of significant intra-annual changes were obtained from the MODIS-based seasonal trend analysis during the period 2001-2011. These classes include different combinations of significant changes in greenness parameters. Approximately 42% of the Abay basin represents significant seasonal trends, out of which 96% represents the dominant eight classes (Table 6 and Figure 6). Almost all vegetated land cover types commonly and dominantly exhibits the seasonal trend characteristics of Class 1, Class 2 and Class3 (Table 6). In addition, Class 4-type seasonal trend is observed mainly over 14% of the woodland and 15% of the natural forest in the Abay basin. Seasonal trend classes of Class 5, Class 6 and Class 8 occur in small proportion of each vegetated land cover types. A particular land cover can exhibit different seasonal trend characteristic. For example, 40%, 27%, and 18% of the grassland in the Abay basin exhibit the seasonal trend characteristics of Class 1, Class 2 and Class 3, respectively. Class 7-type seasonal trend is observed over 13% of the natural forest area.

Class 1 has an area of 31,664 km^2, which accounts for 16.09% of the total land scape of Abay and 38.28% of all significant pixels ($p < 0.05$) (Table 6). This class represents areas with a significant decreasing trend in peak of annual greenness (Amplitude 1), with no significant changes in overall greenness and time peak greenness during the period 2001 – 2011. Fig. 7 (a) shows a decrease in greenness in the wet season (June, July, August, September), but an increase in greenness in the dry season (January, February, March, April). Class 2 represents significant decreases in overall greenness and annual peak greenness, with no significant changes in other greenness parameters (Table 6). Fig. 7 (b) shows the seasonal curves of NDVI (2-year average) for Class 2. The maximum difference between the two curves occurs in August, whereas the minimum difference occurs in February and November. NDVI values for both curves are above 0.6. Class 3 has an area of 11,408 km^2 and describes 16.21% of all significant seasonal trend and 6.8% of the basin total area (Table 6). Class 3 represents areas with a significantly negative trend in overall greenness (Amplitude 0) and no significant change in any of the other greenness parameters, producing curve that is decreased uniformly throughout the year. The NDVI values at all months remain above 0.7 throughout the year. About 34% of the natural forest corresponds to Class 3 type of seasonal trend. Thus, the change in overall greenness may indicate a decrease in vegetation density without complete removal forest. Class 4 describes about 8% of all significant trends and covers an area of 6525 km^2 (Table 6). Class 4 includes areas that exhibit a

significant increase in Phase 1 (the time of annual peak greenness), but no other significant seasonal trend parameters. Fig. 7 (d) depicts the seasonal curves of Class 4 at the initial (average of 2001 and 2002) and final period (average of 2010 and 2011) of the analysis. This class of seasonal trend exhibits a shift in the timing of annual peak greenness to an earlier time of the year. Class 5 represents areas with significant decrease in both Amplitude 0 and Amplitude 1, but significant increase in Phase 1. This type of seasonal trend class is commonly found in Wonbera sub-basins. The NDVI values remain above 0.6 in all months throughout the year. According to Fig. 7(e), the maximum difference between curves occurs between June and November, suggesting that the density of land cover type causing this difference might have been reduced. Class 6 represents areas with a significantly negative trend in Phase 1 and no significant change in any of the other greenness parameters. This class is mostly found in North Gojam sub-basin and it is characterized by lower NDVI values throughout the year as compared to the NDVI values of other classes. Class 7 exhibits significant decrease in overall greenness and significant increase in the time peak annual greenness. The NDVI values at all months remain above 0.7 throughout the year, making it similar with that of Class 3. Both Class 3 and Class 7 are mostly located in Didessa sub-basin. Class 8 represents areas with significant decrease in annual peak greenness and significant increase in time of peak annual greenness. These changes are noticeable in Fig. 7(h). The annual peak greenness observed in the initial state (2001/2002) decreased by approximately 0.2NDVI units between July and October as compared to the final state (2010/2011).

3.3 Trend break analysis

3.3.1 GIMMS NDVI

Trend break analysis in the inter-annual data series

The tread break analysis of ROIs shown in Figure 8 illustrates different trend behavior within a longer time series of GIMMS data. Trends are not always continuously increasing or decreasing but can change over time. For example, ROI #2 (Fig.8(b)) and ROI #4 (Fig.8(d)) represent gradual browning and greening trends, respectively, over the entire study period, while ROI #1 and ROI #3 describe abrupt browning and greening, respectively. ROI #1 characterized by trend breaks at December 1989 and August 1997 and ROI #3 shows a trend break at April 1998. Thus,

the trend break analysis assisted identification of several change periods which might otherwise been overlooked through a commonly assumed fixed change trajectory analysis.

Trend break analysis in the HANTS seasonality parameters

Trend break analysis was performed on the harmonic shape parameters to identify the time when abrupt change occurred. No significant break points were detected based on OLS-based MOSUM test for structural change using BFAST. However, through visual interpretation it is possible to identify trend break points. For example, Class 2 and Class 5 showed a sharp increase in Phase 1 between 1988 and 1998 and sharp decrease afterwards (Fig. 9).

3.3.2 MODIS NDVI

The trend-break analysis did not indicate significant trend breaks using the BFAST approach in all of the sampled areas (Fig. 10) suggesting that vegetation activity in Abay basin showed a monotonic increasing or decreasing behavior. Slowly acting processes such as land management practices or land degradation may cause such monotonic changes in the time series.

ROI#1 and ROI#2 are similar in representing areas of significant monotonic decreasing trend in vegetation condition but different in the reasons behind the trend. ROI#1 is located in Didessa sub-basin and the main reason for the observed decreasing trend is due to the decrease in woody vegetation density by human activity. ROI#2 is located in Beless sub-basin and forest fire is the main cause for the observed decrease in vegetation condition. Both ROI#3 and ROI#4 represent areas of significant increasing trend in vegetation condition. Trend-break is observed in the seasonal component of the NDVI time series, but not in the trend component (Fig. 10(c)). The seasonal component the NDVI time series in ROI#3 has changed since 2008. This indicates that new activities causing increased greenness are occurring in the area. ROI#4 is located in between Welaka and Jemma sub-basins.

Trend-break analysis in the HANTS seasonality parameters

Although there is a significant monotonic increasing or decreasing trend, no significant break points were identified in any of the greenness parameters based on OLS-based MOSUM test. The trends in overall greenness and annual peak greenness appear to be continuously increasing or decreasing without trend breaks. However, Phase1 in Class 5, Class 6 and Class 8 shows a non-significant trend breaks (Fig. 11). The time of annual peak greenness has increased since the year 2007.

4. Discussion

4.1 GIMMS-based inter-annual and seasonal trends

Vegetation trend analysis using the monthly GIMMS NDVI revealed a significant increase in the vegetation condition over 41.15% of the Abay basin for the period 1982-2006. Several studies have also reported widespread greening and increased vegetation growth and productivity for various areas of the world particularly in the Northern Hemisphere (Nemani et al., 2003;Slayback et al., 2003;Zhou et al., 2001). The north western and western parts of the basin that exhibited positive NDVI change are mainly covered with lowland vegetation such as woodland and shrubland. These areas are used for traditional uses such as shifting cultivation and livestock rearing, by the small indigenous population. One key characteristic of these areas is the periodic burning of vegetation, as it is evident from fire scares visible on Landsat images. The reason for this burning is to get a very good grass for the next season for livestocks. Thus, the positive NDVI trend of these areas could be attributed to a decreasing trend of burning of vegetation. However, detailed investigation of these areas is crucial to be able to attribute the trend to particular cause.

The basin is characterized not only by significant inter-annual variation, but also by a significant trend in seasonality. More than half (59.52%) of land areas exhibited a significant trend in seasonality over the 25 year time period measured (1982-2006). Thus, a trend in seasonality is not a rare occurrence in Abay basin. Eastman et al. (2013) in their global study also concluded that a significant trend in seasonality is not a rare occurrence. Areas with significantly positive trend in mean annual NDVI (Amplitude 0) were found to be the dominant seasonal trend class, which accounts for 16.85% of all significantly trending areas and 10.03% of the total land area. The majority of this seasonal trend class occurs in areas of woodland and shrubland. A significant increase in mean annual NDVI without significant changes in any of the other harmonic shape parameters, as Amplitude 0 correlates with annual integrated NDVI rescaled to a mean value. Integrated NDVI correlates strongly with annual gross primary productivity (Reed et al., 1994). Thus increasing trend in Amplitude 0 would implyincreased productivity uniformly throughout the year. It appears that woodland and shrubland areas of Abay basin are experiencing a consistent increase in productivity throughout the year. ,This result is consistent

with previous findings over the African Sahel region (Eklundh and Olsson, 2003; Anyamba & Tucker, 2005; Olsson et al., 2005; Heumann et al., 2007)

The most likely driving factor of monotonic greening or browning could be changes in growth-limiting climatologies (Nemani et al., 2003), broad-scale land management practices, and persistent land use change driven by settlements (e.g., cropland expansion and urbanization) (Ramankutty et al., 2007). Strongest indication for greening in agricultural expansion areas such as Fincha and Belles sub-basins is most likely attributable to improved agricultural techniques. Abrupt browning could be caused by logging followed by regrowth or the already existed vegetation decline in some places might have amplified by a period of persistently poor rains. However, abrupt greening could be caused by wet period induced by El Nino/La Nina Southern Oscillation warming events such as ENSO 1986/87, 1994/95, and 1997/98. The year 1997/1998 was identified as a trend break point using the Pettitt test. Thus, greening might represent recovery from drought or other disturbances such as forest fire (Anyamba and Tucker, 2005;Heumann et al., 2007;Olsson et al., 2005). Greening as a result of land management such as forest plantation cannot be traced with GIMMS data, as most of the plantations are taking place in the area at local scale and individual farm level. Finally, although the GIMMS data sets have been thoroughly corrected (Tucker et al., 2005), AVHRR satellite platform changes could potentially cause trend breaks within the time series. The detected trend break time was compared with the time of AVHRR platform change (1985, 1988, 1994, 1995, 2000 and 2004) (Tucker et al., 2005) and it was found that that they are different. With regard to attribution of vegetation trend to the drivers, the courser scale analysis only provides indications for more focused analysis, because the driving factors might act on a local scale much smaller than the resolution of GIMMS NDVI (i.e. 8 km). Thus, based on the information obtained from this courser scale analysis area specific attribution of the increase in greenness to its causes is required for the Abay basin for the future.

4.2 MODIS-based inter-annual and seasonal trends

The vegetation trend analysis with a spatial resolution of 250 m MODIS (2001-2011) depicted a different perspective from that of 8km spatial resolution of GIMMS data set (1982-2006). About 36% of the UBN/Abay basin showed a significantly browning trend and only 1.19% of the basin showed a significantly greening trend over the period 2001-2011. The majority of the browning

trend comes from Dabus, Belles, Wonbera and Didessa. The MODIS-based vegetation seasonal trend analysis during the period 2001-2011 revealed four conspicuous vegetation changes, which accounts for 86% of all significant pixels: (1) a change in the greenness pattern from a strong annual cycle to strong semi-annual vegetation cycle, indicating significant changes from shrubland/woodland vegetation to double cropping (irrigation); (2) a decrease in both overall greenness and annual peak greenness; (3) degradation of vegetation without complete removal (e.g. ROI#3); and (4) a change from semi-annual vegetation cycle to strong annual vegetation cycle. These areas could have been masked if only the inter-annual vegetation trend analysis was performed. Thus, carrying out intra-annual trend analysis at medium resolution (250 m) would be helpful since most of the deforestations for the purpose of small scale irrigation are operating at local scale. However, a mere identification of areas with significant intra-annual vegetation change is not enough for monitoring of vegetation condition. Attribution of the observed categories of intra-annual changes to the driving factors based on detailed field observation is also important.

The BFAST approach of the trend break analysis indicated a monotonic increasing or decreasing vegetation condition without any significant trend breaks. The greening tend observed from GIMMS data set might have been reversed into browning trend suggesting a localized decline in vegetation activity during the period 2004-2006. This result is consistent with the findings of de Jong et al. (2013b), who explained a trend reversal into browning trend not confined to single geographical region, but extended across all continents. In the 1980s and 1990s the Northern Hemisphere was found to become greener (Nemani et al., 2003;Zhou et al., 2001). The impact of sensor degradation on trends in MODIS NDVI (Wang et al., 2012) could be one cause for recent browning trend in the basin. Some anthropogenic factors could also be attributed to the observed recent browning trend in the basin. One of the possible drivers of browning in the northwest part of the basin especially in Rahad and some part Dinder sub-basins could be intra-regional resettlement (i.e. people from the same area with kin relations in the same locality) and its associated deforestation for cropland expansion (Dixon and Wood, 2007;Lemenih et al., 2014). The Amhara regional government of Ethiopia initiated ‘voluntary’ resettlement scheme since 2003 for the most chronically food insecure people from all zones of the region to potentially more productive, fertile and less populated parts such as Metema, Quara, Tach Armacheho and

Tegede woredas of North Gondar administrative zone (NCFSE, 2003). In the Belles sub-basin land preparation for small to medium scale irrigation schemes could initially cause a decline in vegetation trend, but after a while the browning trend might be reversed to greening trend. Currently, private and government agricultural investments are underway in this sub-basin. Thus, the decreasing trend of vegetation greenness in the Belles sub-basin can be largely explained by the de-vegetation during land preparation for sugarcane plantation particularly in Alefa and Jawi weredas from Amhara regional state and Pawe and Dandur weredas from Benshagul Gumz regional states of Ethiopia. Such big croplands could contribute to the browning in the initial stage and to the greening once the cropland is established.

4. Conclusions

There are two notable features of long-term trend analysis conducted on monthly GIMMS NDVI data from 1982 to 2006. First, based on robust trend estimators (Theil-Sen slope) most part of the Upper Blue Nile basin (~77%) showed a positive trend in monthly NDVI with a mean rate of 0.0015 NDVI units (3.77% yr^{-1}), out of which 41.15% of the basin area depicted significant increases ($p < 0.05$) with a mean rate of 0.0023 NDVI units (5.59% yr^{-1}). Second, the upward trend (positive change) in NDVI is most intense in the northwestern and downward trend (negative change) in NDVI is intense in the southern and eastern part of the basin. Areas showing high NDVI variability were found to be the ones exhibiting long-term positive trends. The MODIS-based vegetation trend analysis revealed that about 36% of the UBN/Abay basin shows a significantly browning trend ($p < 0.05$) over the period 2001-2011 at an average rate of 0.0768 NDVI yr^{-1} using MODIS 250m spatial resolution. The majority of this browning trend comes from the sub-basins Dabus, Belles, Wonbera, and Didessa. The vegetation activity in the Belles sub basin has decreased at a faster rate (0.082NDVI yr^{-1}) than the other sub-basins. The greening trend observed from the GIMMS data set might have been reversed into browning trend and suggests a localized decline in vegetation activity in recent years. Anthropogenic factors such as resettlement and agricultural expansion could be attributed to the observed greening-to-browning reversal of vegetation conditions in the UBN basin.

Intra-annual trend analysis identified changes in vegetation condition that could have been masked if only the inter-annual vegetation trend analysis was performed. Changes in seasonality was found to be prevalent in the landscape of Upper Blue Nile/Abay basin as more than half (59.52%) of land areas exhibit a significant trend in seasonality over the 25 year time period measured (1982-2006). Only five types of seasonal trends were dominant out of which the largest proportion describes areas that are experiencing a uniform increase in NDVI throughout the year. It appears that woodland and shrubland areas of the basin experienced increase in vegetation productivity resulting from longer growing season. The seasonal trend analysis of MODIS NDVI (2001-2011) also confirmed that seasonal trend is not a rare occurrence in the Abay basin as 42% of the basin represents significant seasonal trends.

Trend break analysis of GIMMS NDVI (1982-2006) showed that trends in vegetation conditions of the UBN basin were found to be not only monotonic, but also abrupt. The step change was detected in 1997/1998 in both inter-annual and intra-annual vegetation time series analysis. Thus, the trend break analysis assisted identification of several change periods which might otherwise be overlooked through a commonly assumed fixed change trajectory analysis. On the other hand, the trend break analysis performed on MODIS NDVI (2001-2011) using BFAST approach were not able to detect trend breaks suggesting that vegetation activity in Abay basin showed a monotonic increasing or decreasing behavior. Slowly acting processes such as land management practices or land degradation may cause such monotonic changes in the time series.

This study concludes that integrated analysis of inter-annual & intra-annual trend based on NDVI from GIMMS and MODIS revealed the following points:

- The greening trend of vegetation condition was followed by browning trend since mid-2000s in the Abay basin. Thus, there is an urgent need in increasing the vegetation activities in the basin.
- Intra-annual trend analysis was found to be very useful in identifying changes in vegetation condition that could have been masked if only the inter-annual vegetation trend analysis was performed.
- The MODIS-based intra-annual trend analysis revealed trends that were more linked to human activities;

Acknowledgements

The authors are also grateful to the Netherlands Fellowship Programmes (NFP) for providing financial support to the first author. We also wish thank the NASA Global Inventory Modeling and Mapping Studies (GIMMS) group for producing and sharing the AVHRR GIMMS NDVI data sets, NASA/MODIS Land Discipline Group for sharing the MODIS LAND data, and the community of the R statistical software for providing a wealth of functionality. We also thank the anonymous reviewers whose comments helped to improve the manuscript.

References

Angert, A., Biraud, S., Bonfils, C., Henning, C., Buermann, W., Pinzon, J., Tucker, C., and Fung, I.: Drier summers cancel out the CO2 uptake enhancement induced by warmer springs, Proceedings of the National Academy of Sciences of the United States of America, 102, 10823-10827, 2005.

Anyamba, A., and Tucker, C.: Analysis of Sahelian vegetation dynamics using NOAA-AVHRR NDVI data from 1981–2003, Journal of Arid Environments, 63, 596-614, 2005.

Bai, Z. G., Dent, D. L., Olsson, L., and Schaepman, M. E.: Proxy global assessment of land degradation, Soil use and management, 24, 223-234, 2008.

Bala, G., Joshi, J., Chaturvedi, R. K., Gangamani, H. V., Hashimoto, H., and Nemani, R.: Trends and variability of AVHRR-derived NPP in India, Remote Sens., 5, 810-829, 2013.

Baldocchi, D., Falge, E., Gu, L., Olson, R., Hollinger, D., Running, S., Anthoni, P., Bernhofer, C., Davis, K., and Evans, R.: FLUXNET: A new tool to study the temporal and spatial variability of ecosystem-scale carbon dioxide, water vapor, and energy flux densities, Bulletin of the American Meteorological Society, 82, 2415-2434, 2001.

Buenemann, M., Martius, C., Jones, J., Herrmann, S., Klein, D., Mulligan, M., Reed, M., Winslow, M., Washington-Allen, R., and Lal, R.: Integrative geospatial approaches for the comprehensive monitoring and assessment of land management sustainability: rationale, potentials, and characteristics, Land Degradation & Development, 22, 226-239, 2011.

De Beurs, K., Wright, C., and Henebry, G.: Dual scale trend analysis for evaluating climatic and anthropogenic effects on the vegetated land surface in Russia and Kazakhstan, Environ. Res. Lett., 4, 045012, 2009.

de Jong, R., de Bruin, S., de Wit, A., Schaepman, M. E., and Dent, D. L.: Analysis of monotonic greening and browning trends from global NDVI time-series, Remote Sensing of Environment, 115, 692-702, 2011.

de Jong, R., Verbesselt, J., Schaepman, M. E., and Bruin, S.: Trend changes in global greening and browning: contribution of short-term trends to longer-term change, Glob. Change Biol., 18, 642-655, 2012.

de Jong, R., Schaepman, M. E., Furrer, R., Bruin, S., and Verburg, P. H.: Spatial relationship between climatologies and changes in global vegetation activity, Global change biology, 19, 1953-1964, 2013a.

de Jong, R., Verbesselt, J., Zeileis, A., and Schaepman, M. E.: Shifts in global vegetation activity trends, Remote Sens., 5, 1117-1133, 2013b.

De Wit, A., and Su, B.: Deriving phenological indicators from SPOT-VGT data using the HANTS algorithm, 2nd international SPOT-VEGETATION user conference, 2005, 195-201,

Dixon, A. B., and Wood, A. P.: Local institutions for wetland management in Ethiopia: Sustainability and state intervention, Community-based water law and water resource management reform in developing countries, 130-145, 2007.
Dregne, H., Kassas, M., and Rozanov, B.: A new assessment of the world status of desertification, Desertification Control Bulletin, 20, 6-18, 1991.
Eastman, J. R., Sangermano, F., Ghimire, B., Zhu, H., Chen, H., Neeti, N., Cai, Y., Machado, E. A., and Crema, S. C.: Seasonal trend analysis of image time series, International Journal of Remote Sensing, 30, 2721-2726, 2009.
Eastman, J. R., Sangermano, F., Machado, E. A., Rogan, J., and Anyamba, A.: Global trends in seasonality of normalized difference vegetation index (NDVI), 1982–2011, Remote Sens., 5, 4799-4818, 2013.
Fensholt, R., Rasmussen, K., Nielsen, T. T., and Mbow, C.: Evaluation of earth observation based long term vegetation trends—Intercomparing NDVI time series trend analysis consistency of Sahel from AVHRR GIMMS, Terra MODIS and SPOT VGT data, Remote Sensing of Environment, 113, 1886-1898, 2009.
Gallo, K., Ji, L., Reed, B., Eidenshink, J., and Dwyer, J.: Multi-platform comparisons of MODIS and AVHRR normalized difference vegetation index data, Remote Sensing of Environment, 99, 221-231, 2005.
Gao, P., Mu, X.-M., Wang, F., and Li, R.: Changes in streamflow and sediment discharge and the response to human activities in the middle reaches of the Yellow River, Hydrology and Earth System Sciences, 15, 1-10, 2011.
Gilbert, R. O.: Statistical methods for environmental pollution monitoring, John Wiley & Sons, Pacific Northwest Lab., Richland, WA (USA), 336 pp., 1987.
Godfray, H. C. J., Beddington, J. R., Crute, I. R., Haddad, L., Lawrence, D., Muir, J. F., Pretty, J., Robinson, S., Thomas, S. M., and Toulmin, C.: Food security: the challenge of feeding 9 billion people, science, 327, 812-818, 2010.
Guerreiro, S. B., Kilsby, C. G., and Serinaldi, F.: Analysis of time variation of rainfall in transnational basins in Iberia: abrupt changes or trends?, International Journal of Climatology, 34, 114-133, 2014.
Harris, I., Jones, P., Osborn, T., and Lister, D.: Updated high-resolution grids of monthly climatic observations–the CRU TS3. 10 Dataset, International Journal of Climatology, 34, 623-642, 2014.
Harris, J. W., and Stöcker, H.: Handbook of mathematics and computational science, Springer, New York, USA, 1028 pp., 1998.
Henebry, G. M.: Global change: carbon in idle croplands, Nature, 457, 1089-1090, 2009.
Heumann, B. W., Seaquist, J., Eklundh, L., and Jönsson, P.: AVHRR derived phenological change in the Sahel and Soudan, Africa, 1982–2005, Remote Sensing of Environment, 108, 385-392, 2007.
Hoaglin, D. C., Mosteller, F., and Tukey, J. W.: Understanding robust and exploratory data analysis, Wiley New York, 1983.
Holben, B. N.: Characteristics of maximum-value composite images from temporal AVHRR data, International Journal of Remote Sensing, 7, 1417-1434, 1986.
Huete, A., Didan, K., Miura, T., Rodriguez, E. P., Gao, X., and Ferreira, L. G.: Overview of the radiometric and biophysical performance of the MODIS vegetation indices, Remote sensing of environment, 83, 195-213, 2002.
Jakubauskas, M. E., Legates, D. R., and Kastens, J. H.: Harmonic analysis of time-series AVHRR NDVI data, Photogrammetric Engineering and Remote Sensing, 67, 461-470, 2001.
Karlsen, S. R., Solheim, I., Beck, P. S., Høgda, K. A., Wielgolaski, F. E., and Tømmervik, H.: Variability of the start of the growing season in Fennoscandia, 1982–2002, International Journal of Biometeorology, 51, 513-524, 2007.
Kearney, J.: Food consumption trends and drivers, Philosophical transactions of the royal society B: biological sciences, 365, 2793-2807, 2010.
Kendall, M. G.: Rank correlation methods, Charles Griffen & Company, London, 160 pp., 1948.

Landin, M. G., and Bosart, L. F.: The diurnal variation of precipitation in California and Nevada, Monthly weather review, 117, 1801-1816, 1989.
Legates, D. R., and Willmott, C. J.: Mean seasonal and spatial variability in gauge-corrected, global precipitation, International Journal of Climatology, 10, 111-127, 1990.
Lemenih, M., Kassa, H., Kassie, G., Abebaw, D., and Teka, W.: Resettlement and woodland management problems and options: A case study from northwestern Ethiopia, Land Degradation & Development, 25(4), 305-318, 2014.
Mann, H. B.: Nonparametric tests against trend, Econometrica: Journal of the Econometric Society, 13, 245-259, 1945.
Metternicht, G., Zinck, J., Blanco, P., and Del Valle, H.: Remote sensing of land degradation: Experiences from Latin America and the Caribbean, Journal of environmental quality, 39, 42-61, 2010.
Nagol, J. R., Vermote, E. F., and Prince, S. D.: Effects of atmospheric variation on AVHRR NDVI data, Remote Sensing of Environment, 113, 392-397, 2009.
NCFSE, N. C. f. F. S. i. E.: Voluntary Resettlement Programme (Access to improved land), vol. II, Addis Ababa, Ethiopia, 2003.
Neeti, N., and Eastman, J. R.: A contextual mann-kendall approach for the assessment of trend significance in image time series, Transactions in GIS, 15, 599-611, 2011.
Nemani, R. R., Keeling, C. D., Hashimoto, H., Jolly, W. M., Piper, S. C., Tucker, C. J., Myneni, R. B., and Running, S. W.: Climate-driven increases in global terrestrial net primary production from 1982 to 1999, science, 300, 1560-1563, 2003.
Olsson, L., Eklundh, L., and Ardö, J.: A recent greening of the Sahel—trends, patterns and potential causes, Journal of Arid Environments, 63, 556-566, 2005.
Parmesan, C., and Yohe, G.: A globally coherent fingerprint of climate change impacts across natural systems, Nature, 421, 37-42, 2003.
Pettitt, A.: A non-parametric approach to the change-point problem, Applied statistics, 28, 126-135, 1979.
Ramankutty, N., Gibbs, H. K., Achard, F., Defries, R., Foley, J. A., and Houghton, R.: Challenges to estimating carbon emissions from tropical deforestation, Global Change Biology, 13, 51-66, 2007.
Reed, B. C., Brown, J. F., VanderZee, D., Loveland, T. R., Merchant, J. W., and Ohlen, D. O.: Measuring phenological variability from satellite imagery, Journal of Vegetation Science, 5, 703-714, 1994.
Richardson, A. D., Black, T. A., Ciais, P., Delbart, N., Friedl, M. A., Gobron, N., Hollinger, D. Y., Kutsch, W. L., Longdoz, B., and Luyssaert, S.: Influence of spring and autumn phenological transitions on forest ecosystem productivity, Philosophical Transactions of the Royal Society B: Biological Sciences, 365, 3227-3246, 2010.
Roerink, G., Menenti, M., and Verhoef, W.: Reconstructing cloudfree NDVI composites using Fourier analysis of time series, International Journal of Remote Sensing, 21, 1911-1917, 2000.
Sen, P. K.: Estimates of the regression coefficient based on Kendall's tau, Journal of the American Statistical Association, 63, 1379-1389, 1968.
Shukla, M., Lal, R., and Ebinger, M.: Determining soil quality indicators by factor analysis, Soil and Tillage Research, **87**, 194-204. DOI: 110.1016/j.still.2005.1003.1011, 2006.
Slayback, D. A., Pinzon, J. E., Los, S. O., and Tucker, C. J.: Northern hemisphere photosynthetic trends 1982–99, Global Change Biology, 9, 1-15, 2003.
Sparks, T. H., Menzel, A., and Stenseth, N. C.: European cooperation in plant phenology, Clim Res, 39, 175-177, 2009.
Thiel, H.: A rank-invariant method of linear and polynomial regression analysis, Part 3, Proceedings of Koninalijke Nederlandse Akademie van Weinenschatpen A, 1950, 1397-1412,
Townshend, J. R., and Justice, C. O.: Selecting the spatial resolution of satellite sensors required for global monitoring of land transformations, International Journal of Remote Sensing, 9, 187-236, 1988.
Tucker, C. J., Slayback, D. A., Pinzon, J. E., Los, S. O., Myneni, R. B., and Taylor, M. G.: Higher northern latitude normalized difference vegetation index and growing season trends from 1982 to 1999, International journal of biometeorology, 45, 184-190, 2001.

Tucker, C. J., Pinzon, J. E., Brown, M. E., Slayback, D. A., Pak, E. W., Mahoney, R., Vermote, E. F., and El Saleous, N.: An extended AVHRR 8-km NDVI dataset compatible with MODIS and SPOT vegetation NDVI data, International Journal of Remote Sensing, 26, 4485-4498, 2005.
UNEP: Global Environmental Outlook, New York, October, 2007.
Verbesselt, J., Hyndman, R., Newnham, G., and Culvenor, D.: Detecting trend and seasonal changes in satellite image time series, Remote sensing of Environment, 114, 106-115, 2010a.
Verbesselt, J., Hyndman, R., Zeileis, A., and Culvenor, D.: Phenological change detection while accounting for abrupt and gradual trends in satellite image time series, Remote Sensing of Environment, 114, 2970-2980, 2010b.
Verhoef, A., van den Hurk, B. J., Jacobs, A. F., and Heusinkveld, B. G.: Thermal soil properties for vineyard (EFEDA-I) and savanna (HAPEX-Sahel) sites, Agricultural and Forest Meteorology, 78, 1-18, 1996.
Villarini, G., Smith, J. A., Baeck, M. L., Vitolo, R., Stephenson, D. B., and Krajewski, W. F.: On the frequency of heavy rainfall for the Midwest of the United States, Journal of Hydrology, 400, 103-120, 2011.
Vogt, J., Safriel, U., Von Maltitz, G., Sokona, Y., Zougmore, R., Bastin, G., and Hill, J.: Monitoring and assessment of land degradation and desertification: Towards new conceptual and integrated approaches, Land Degradation & Development, 22, 150-165, 2011.
Vuichard, N., Ciais, P., Belelli, L., Smith, P., and Valentini, R.: Carbon sequestration due to the abandonment of agriculture in the former USSR since 1990, Global Biogeochemical Cycles, 22, 10.1029/2008GB003212, 2008.
Walther, G.-R., Post, E., Convey, P., Menzel, A., Parmesan, C., Beebee, T. J., Fromentin, J.-M., Hoegh-Guldberg, O., and Bairlein, F.: Ecological responses to recent climate change, Nature, 416, 389-395, 2002.
Wang, D., Morton, D., Masek, J., Wu, A., Nagol, J., Xiong, X., Levy, R., Vermote, E., and Wolfe, R.: Impact of sensor degradation on the MODIS NDVI time series, Remote Sensing of Environment, 119, 55-61, 2012.
Wang, X. L., and Swail, V. R.: Changes of extreme wave heights in Northern Hemisphere oceans and related atmospheric circulation regimes, Journal of Climate, 14, 2204-2221, 2001.
Wessels, K., Prince, S., Frost, P., and Van Zyl, D.: Assessing the effects of human-induced land degradation in the former homelands of northern South Africa with a 1 km AVHRR NDVI time-series, Remote Sensing of Environment, 91, 47-67, 2004.
Wessels, K., Prince, S., Malherbe, J., Small, J., Frost, P., and VanZyl, D.: Can human-induced land degradation be distinguished from the effects of rainfall variability? A case study in South Africa, Journal of Arid Environments, 68, 271-297, 2007.
Wijngaard, J., Klein Tank, A., and Können, G.: Homogeneity of 20th century European daily temperature and precipitation series, International Journal of Climatology, 23, 679-692, 2003.
Wilks, D. S.: Statistical methods in the atmospheric sciences, Academic press, USA, 2011.
Zhao, M., and Running, S. W.: Drought-induced reduction in global terrestrial net primary production from 2000 through 2009, science, 329, 940-943, 2010.
Zhou, L., Tucker, C. J., Kaufmann, R. K., Slayback, D., Shabanov, N. V., and Myneni, R. B.: Variations in northern vegetation activity inferred from satellite data of vegetation index during 1981 to 1999, Journal of Geophysical Research: Atmospheres (1984–2012), 106, 20069-20083, 2001.

Table 1. Parameters used in HANTS analysis

HANTS parameters	GIMMS		MODIS	
	Single year	Full data set	Single year	Full data set
Number of frequency	0, 1, 2	0, 24, 48	0, 1, 2	0, 23, 46
Invalid data rejection threshold:	0 - 1	0 - 1	0 - 1	0 - 1
Fit error tolerance (FET)	0.1	0.1	0.1	0.1
Maximum iterations (i_{MAX})	6	12	6	12
Minimum retained data points	16	416	15	165

Table 2. Result of linear trend analysis based on Theil-Sen (TS) (median) slope for the monthly GIMMS NDVI data

	Slope		**MK-Z trends**	
Trend estimator	**Positive**	**Negative**	**Significantly +**	**Significantly -**
ΔNDVI/month (Absolute change)	0.0015	0.0007	0.0023	0.0017
% NDVI change/month (Relative change)	0.314	0.159	0.466	0.370
Land area (%)	76.85	23.15	41.15	4.60

Absolute change refers to the median slope; Relative change = (median slope/multi-year mean)*100

Table 3. The percentage of sub-basin's significant trend out of the total area of significant trend in the basin and the percentage of area significantly increasing or decreasing within sub-basins are shown. The result is based on MODIS-based analysis. The locations of the sub-basins can be found in Fig. 8.

Sub-basins	**% of total trend**			**% of sub-basin's area**		
	Insignificant trend	Significantly greening	Significantly browning	Insignificant trend	Significantly greening	Significantly browning
Anger	3.37	0.46	5.27	52.96	0.14	46.90
Belles	3.77	1.12	13.50	32.90	0.18	66.91
Beshilo	9.78	18.23	0.97	91.65	3.22	5.13
Dabus	8.76	5.07	14.27	51.68	0.56	47.76
Didessa	9.28	1.76	11.48	58.64	0.21	41.15
Dinder	6.78	0.18	9.19	56.54	0.03	43.43
Finca	2.66	2.96	0.96	81.62	1.71	16.67
Guder	4.85	7.61	1.15	85.87	2.54	11.59
Jemma	11.48	22.03	1.45	90.25	3.26	6.49
Muger	5.88	12.15	0.86	89.13	3.47	7.40
North Gojam	8.65	12.78	4.76	74.64	2.08	23.28
Rahad	2.64	0.01	7.10	39.59	0.00	60.41
South Gojam	8.43	3.88	8.84	62.37	0.54	37.09
Tana	5.11	1.89	8.11	52.45	0.37	47.18
Welaka	4.82	9.77	0.29	93.24	3.56	3.20
Wonbera	3.74	0.10	11.81	35.86	0.02	64.12
Total	100	100	100	63.05	1.19	35.76

Table 4. Summary statistics of Theil-Sen slope (median trend) for the significantly increasing (greening) and decreasing (browning) trends per sub-basins. Locations of the sub-basins can be found in Fig. 8. The minimum, maximum and mean of significantly browning slopes have negative signs. The result is based on MODIS-based analysis.

Sub-basins	**Significantly greening (Δ NDVI yr^{-1})**			**Significantly browning (Δ NDVI yr^{-1})**		
	Minimum	Maximum	Mean	Minimum	Maximum	Mean
Anger	0.0444	0.0984	0.0612	-0.0336	-0.1740	-0.0768
Belles	0.0456	0.1524	0.0744	-0.0348	-0.1908	-0.0816
Beshilo	0.0420	0.1596	0.0660	-0.0384	-0.1572	-0.0660
Dabus	0.0432	0.1812	0.0768	-0.0372	-0.1764	-0.0744
Didessa	0.0444	0.0984	0.0624	-0.0312	-0.2124	-0.0792
Dinder	0.0372	0.0912	0.0552	-0.0348	-0.1692	-0.0756
Fincha	0.0444	0.1524	0.0732	-0.0372	-0.1656	-0.0708
Guder	0.0420	0.1176	0.0648	-0.0360	-0.1584	-0.0684
Jemma	0.0408	0.1920	0.0660	-0.0348	-0.2016	-0.0660
Muger	0.0432	0.1224	0.0648	-0.0408	-0.1464	-0.0684
North Gojam	0.0372	0.1332	0.0660	-0.0384	-0.1704	-0.0732
Rahad	0.0528	0.0660	0.0600	-0.0384	-0.1620	-0.0756
South Gojam	0.0408	0.1308	0.0636	-0.0356	-0.1836	-0.0768
Tana	0.0444	0.1476	0.0672	-0.0372	-0.2028	-0.0792
Welaka	0.0348	0.1476	0.0660	-0.0420	-0.1488	-0.0636
Wonbera	0.0504	0.1452	0.0696	-0.0336	-0.1884	-0.0792
Total	0.0348	0.1920	0.0660	-0.0312	-0.2124	-0.0768

Table 5. Percent of seasonal trend classes by land cover classes for both GIMMS–based and MODIS-based analysis.

Classes of seasonal trends	Grassland	Shrubland	Woodland	Cropland	Natural Forest	Area (km^2)
GIMMS-based analysis						
Class 1 (Sig. ↑ in A0)	34.78	40.71	25.76	13.79	0.00	19712
Class 2 (Sig. ↑ in A0 & ↓ in P1)	7.97	25.66	40.66	13.08	0.00	18560
Class 3 (Sig. ↑ in A1)	10.87	4.87	1.77	17.06	0.00	6848
Class 4 (Sig. ↓ in A1)	39.86	12.39	4.04	40.19	33.33	18688
Class 5 (Sig. ↓ in P1)	6.52	16.37	27.78	15.89	66.67	14720
MODIS-based analysis						
Class 1 (Sig. ↓ in A1)	39.48	34.89	27.10	45.90	16.76	31664
Class 2 (Sig. ↓ in both A0 and A1)	26.97	28.46	24.08	23.66	12.82	19892
Class 3 (Sig. ↓ in A0)	18.09	18.94	23.62	13.31	34.18	13408
Class 4 (Sig. ↑ in P1)	6.83	7.81	14.18	6.91	15.35	6525
Class 5 (Sig. ↓ in both A0 & A1, & ↑ in P1)	3.32	3.08	3.81	2.77	3.82	2374
Class 6 (Sig. ↓ in P1)	1.48	2.45	1.27	3.29	0.31	2058
Class 7 (Sig. ↓ in A0 and ↑ in P1)	2.05	2.81	3.46	1.75	12.74	2058
Class 8 (Sig. ↓ in A1 and ↑ in P1)	1.78	1.56	2.49	2.41	4.01	1787

Note: The upward arrow (↑) indicates increasing trend and the downward arrow (↓) indicates decreasing trend.
Sig. = Significant ($p < 0.05$), A0 = Amplitude 0, A1= Amplitude 1, P1 = Phase 1.

Table 6. Extent of dominant classes of trends in seasonality from MODIS-based analysis.

Dominant trends in seasonality	Area (km^2)	%of total landscape	% of all significant pixels
Class 1 (Sig. ↓ in A1)	31664.19	16.09	38.28
Class 2 (Sig. ↓ in both A0 and A1)	19891.56	10.11	24.05
Class 3 (Sig. ↓ in A0)	13408.13	6.81	16.21
Class 4 (Sig. ↑ in P1)	6525.94	3.32	7.89
Class 5 (Sig. ↓ in both A0 & A1, & ↑ in P1)	2374.31	1.21	2.87
Class 6 (Sig. ↓ in P1)	2058.44	1.05	2.49
Class 7 (Sig. ↓ in A0 and ↑ in P1)	2057.75	1.05	2.49
Class 8 (Sig. ↓ in A1 and ↑ in P1)	1787.06	0.91	2.16
Not significant	2958.06	1.50	-
Others (small sig. changes)	114063.31	57.96	-

Note: Sig. = Significant at $p < 0.05$, ↓=decreasing, ↑= increasing, A0 = Amplitude 0, A1 = Amplitude 1, P1 = Phase 1.

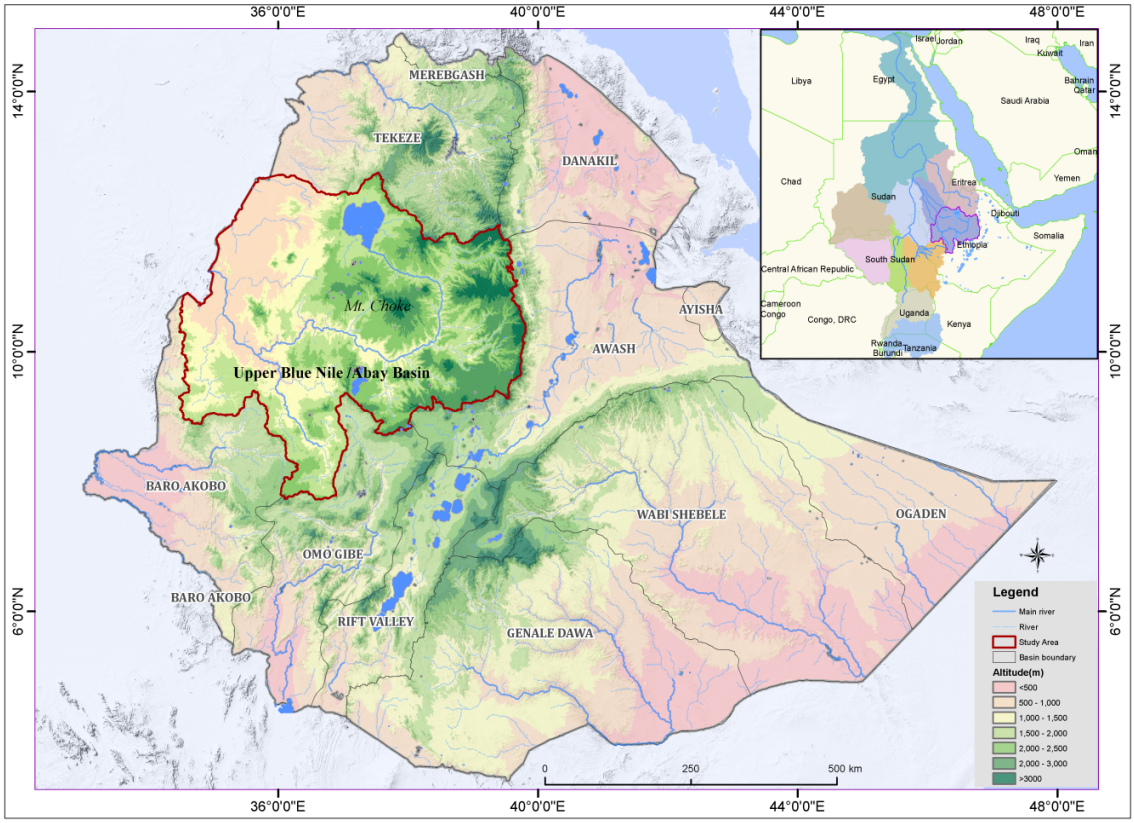

Figure 1. Location map of the study area, Upper Blue Nile/Abay basin, Ethiopia.

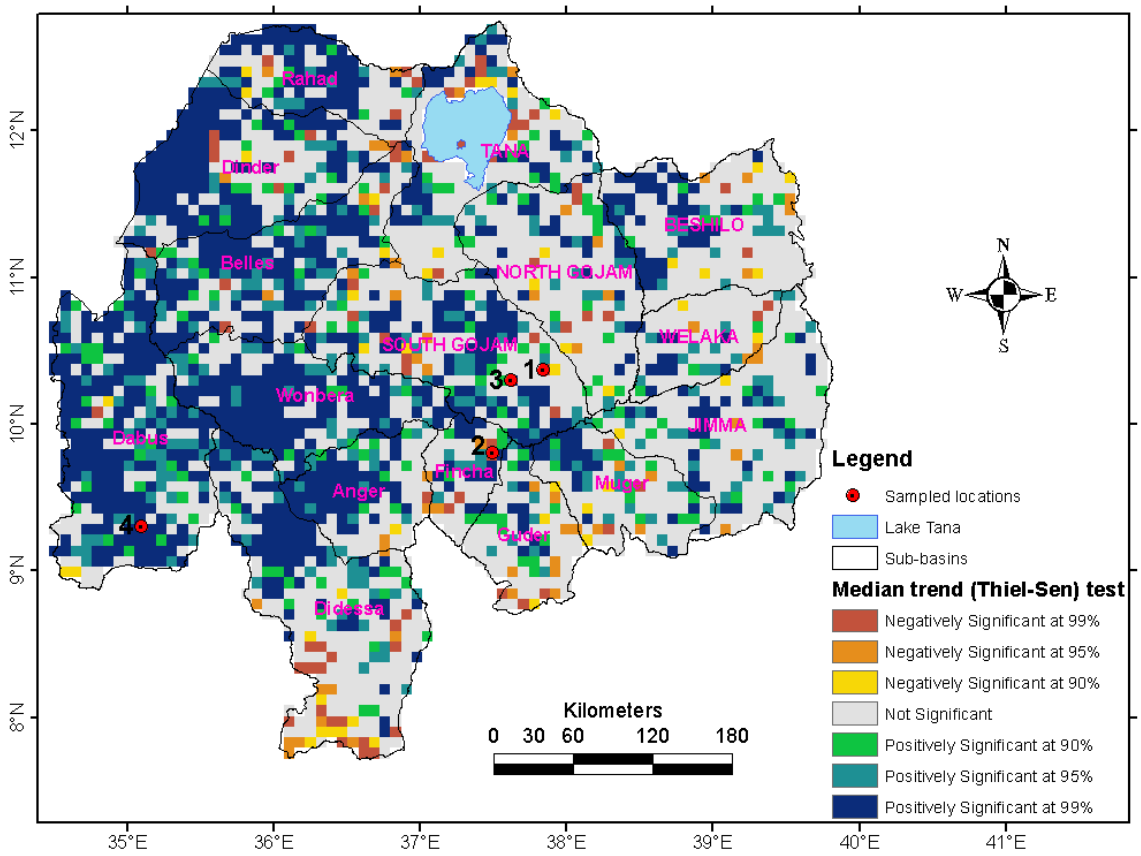

Figure 2. The inter-annual trend in vegetation condition based on GIMMS NDVI in Abay (UBN) basin for the period 1982 to 2006

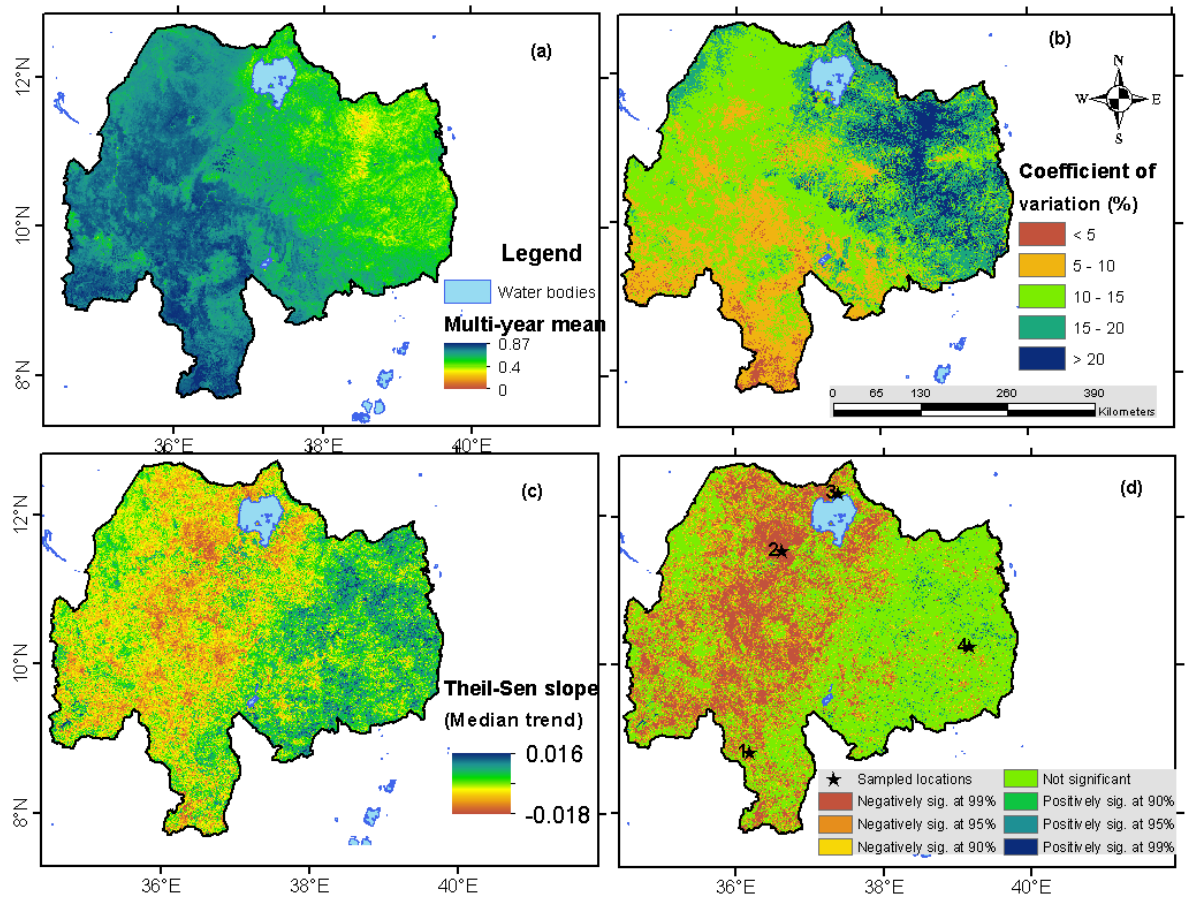

Figure 3. Vegetation cover variability and trends for the Upper Blue Nile (Abay) basin based on MODIS 250m NDVI (MOD13Q1) for the period (2001-2011): (a) multi-year mean monthly NDVI; (b) coefficient of variation of monthly NDVI; (c) Theil-Sen slope (ΔNDVI/month); and (d) Mann-Kendall significance test of the trend test.

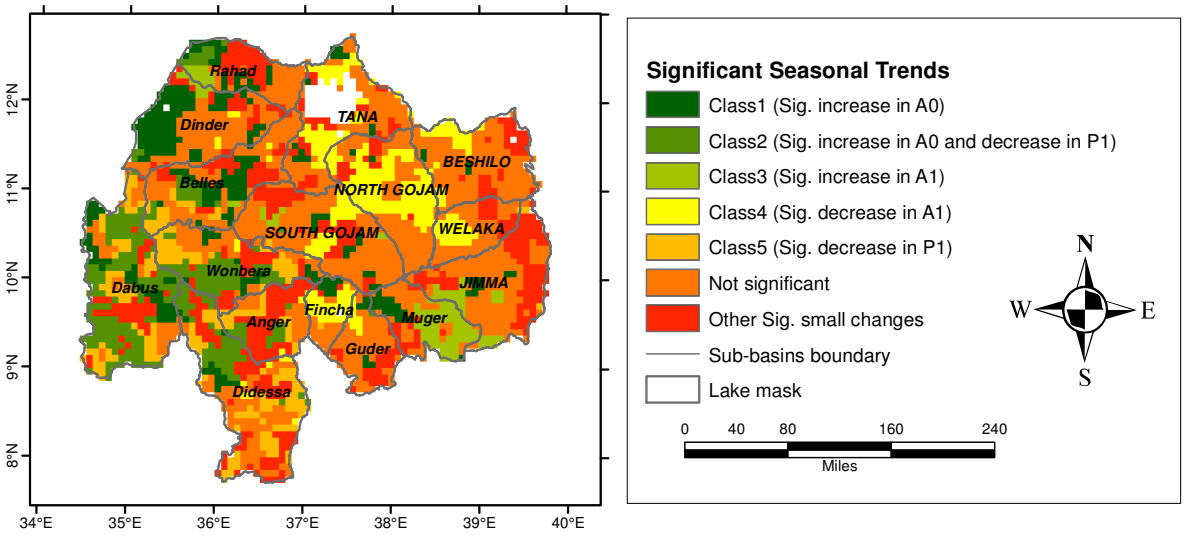

Figure 4. The five most prevalent classes of significant seasonal trends in GIMMS NDVI (1982-2006): Class 1 shows significant increases in Amplitude 0 (Mean NDVI); Class 2 shows significant increases in Amplitude 0 and decrease in Phase 1 (the timing of annual peak greenness) together; Class 3 shows significant increases in Amplitude 1 (increase in the difference between minimum and maximum NDVI without affecting the mean); Class 4 shows significant decreases in Amplitude 1; and Class 5 shows significant decreases in Phase 1.

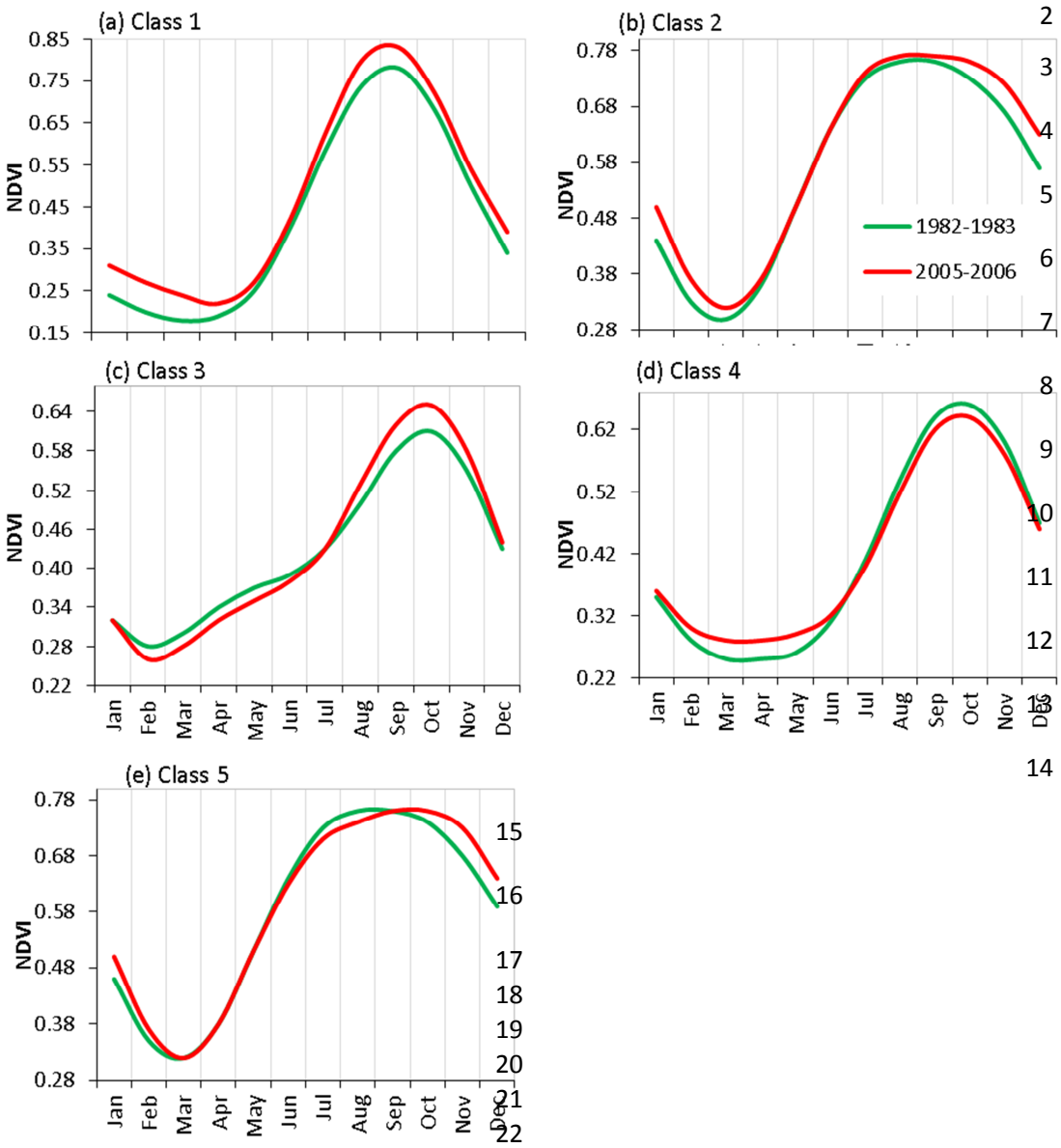

Figure 5. Seasonal curves representative of each of the major trend classes from the 1982–2006 series: the green curve represents the characteristic seasonal curve at the beginning of the series (mean value of 1982 and 1983) while the red curve represents the characteristic seasonal curve at the end of the series (mean value of 2005 and 2006).

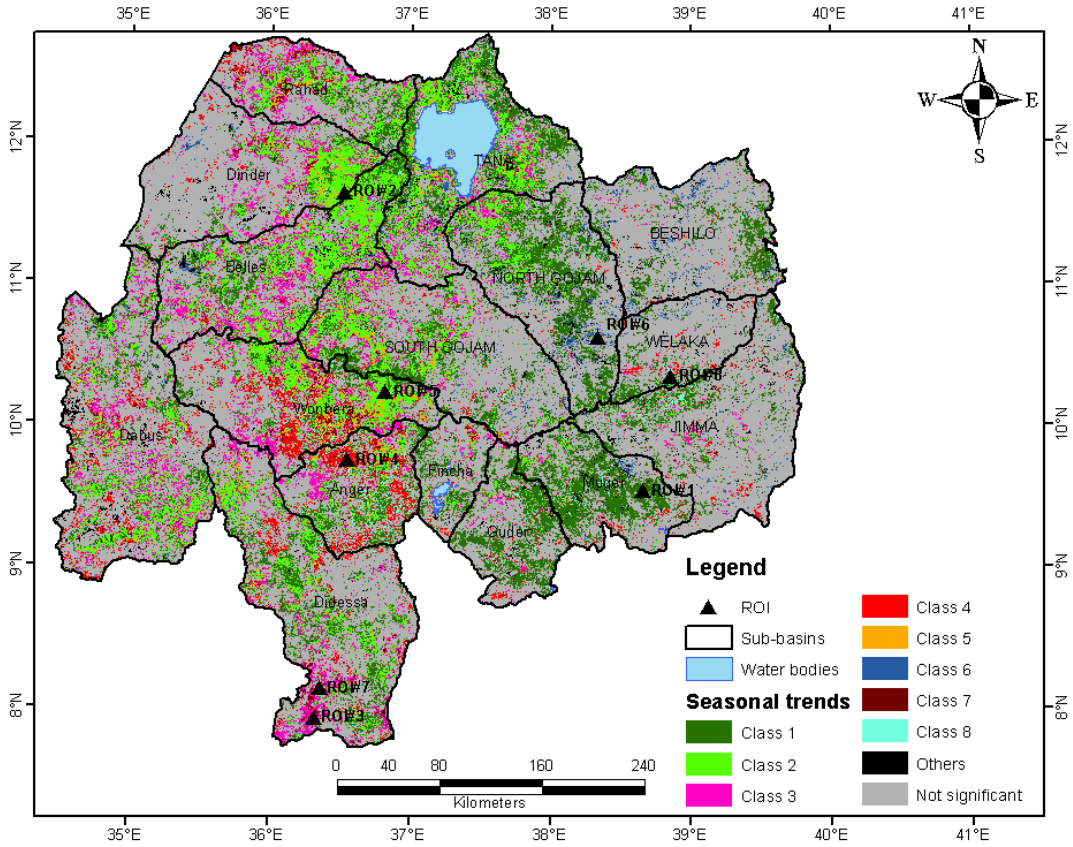

Figure 6. Most prevalent classes of significant seasonal trends of monthly 250m MODIS NDVI (MOD13Q1) for the Upper Blue Nile/Abay basin from 2001 to 2011.

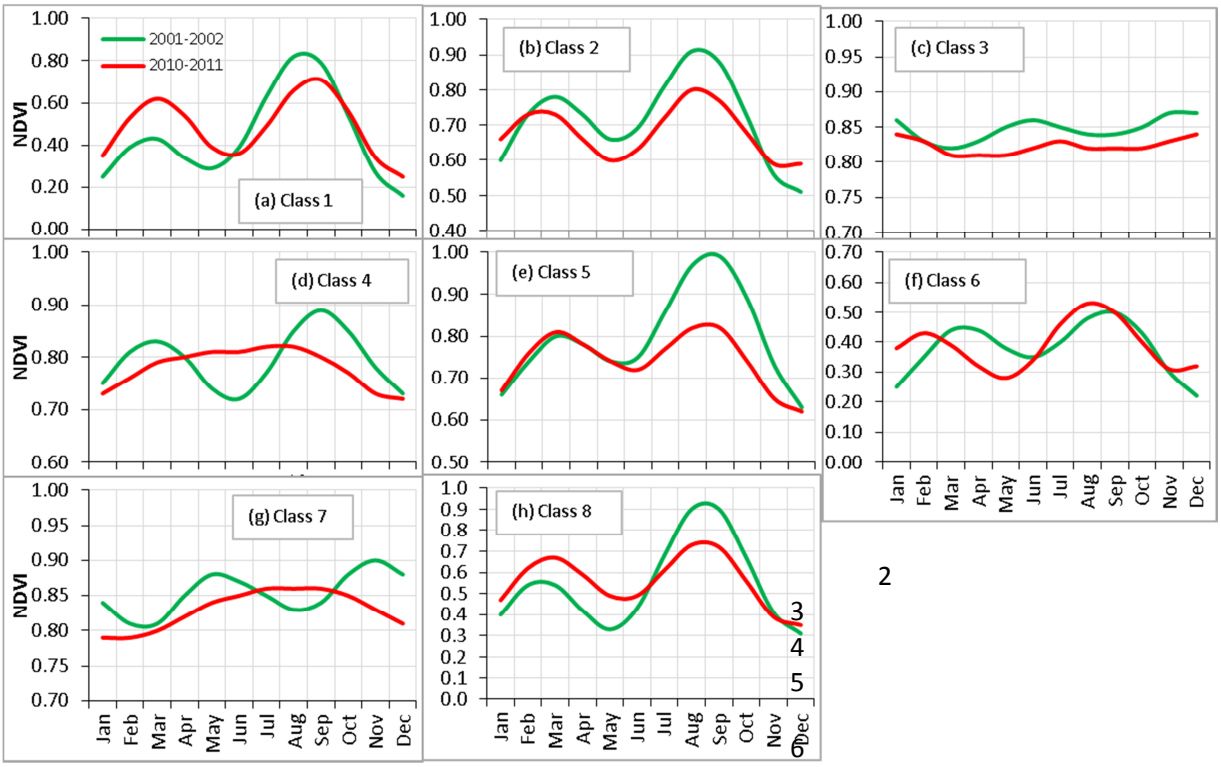

Figure 7. Fitted seasonal curves for 2001-2002 in green and 2010-2011 in red, derived from trends over the complete series. The intra-annual variations of generalized monthly NDVI over the first and last two-year periods of the time series (2001–2002 and 2010–2011) are shown for the 8 ROIs selected based on the amplitude composite images (Fig. 8).

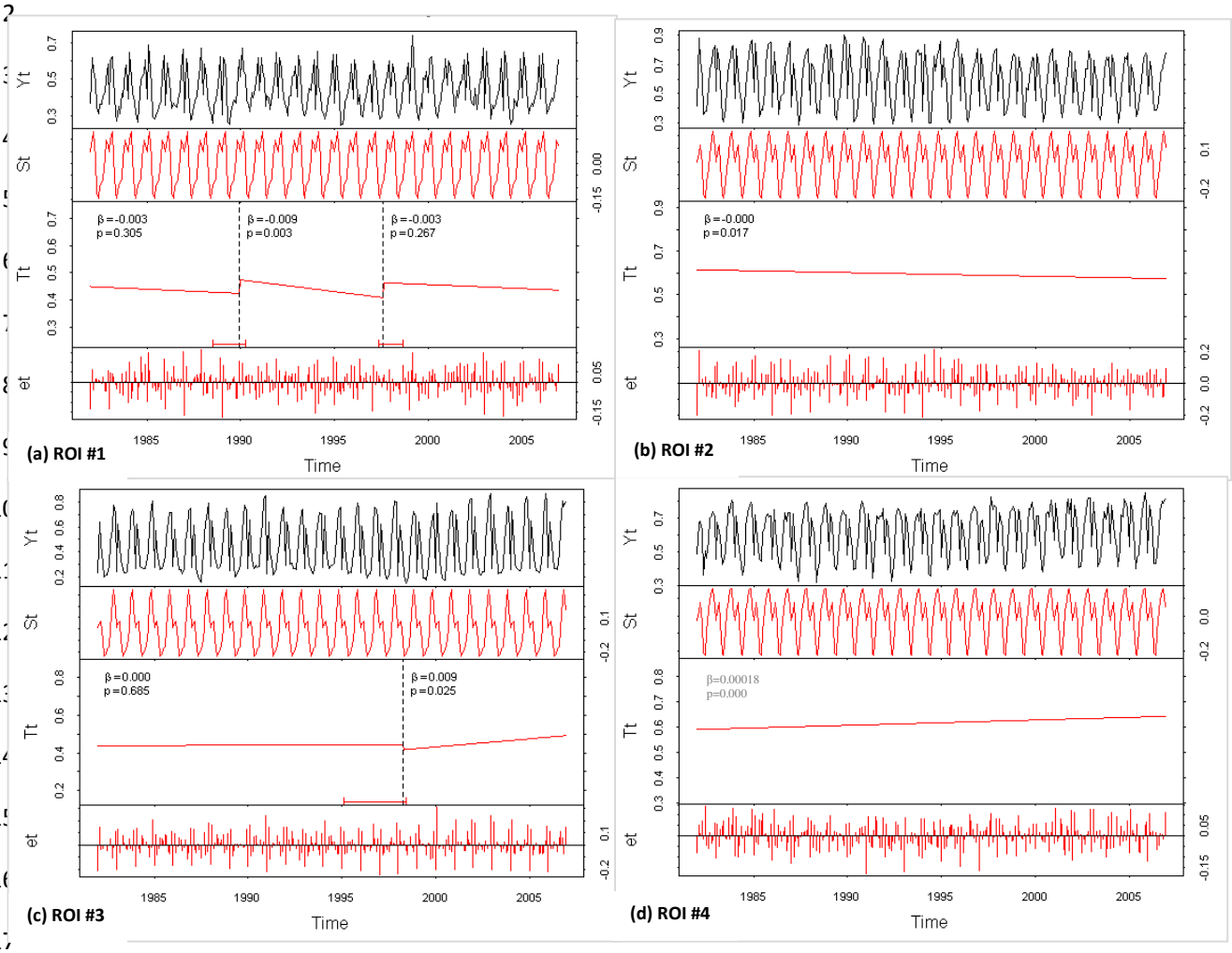

Figure 8. Examples of decomposition and trend break analysis of monthly GIMMS NDVI time series (1982-2006) for sampled region of interests (ROIs) of increasing trend (ROI #1 and ROI #2) and decreasing trend (ROI #3 and ROI #4) generated by BFAST approach. The top panel in every plot shows the NDVI data, whereas the other three panels depict the individual components after decomposition. The seasonal (S_t) and remainder (e_t) components have zero mean while the trend component (T_t) shows the trend in NDVI. The slope coefficients (β) and the significance levels (P) at α value of 0.05 for each segment are given.

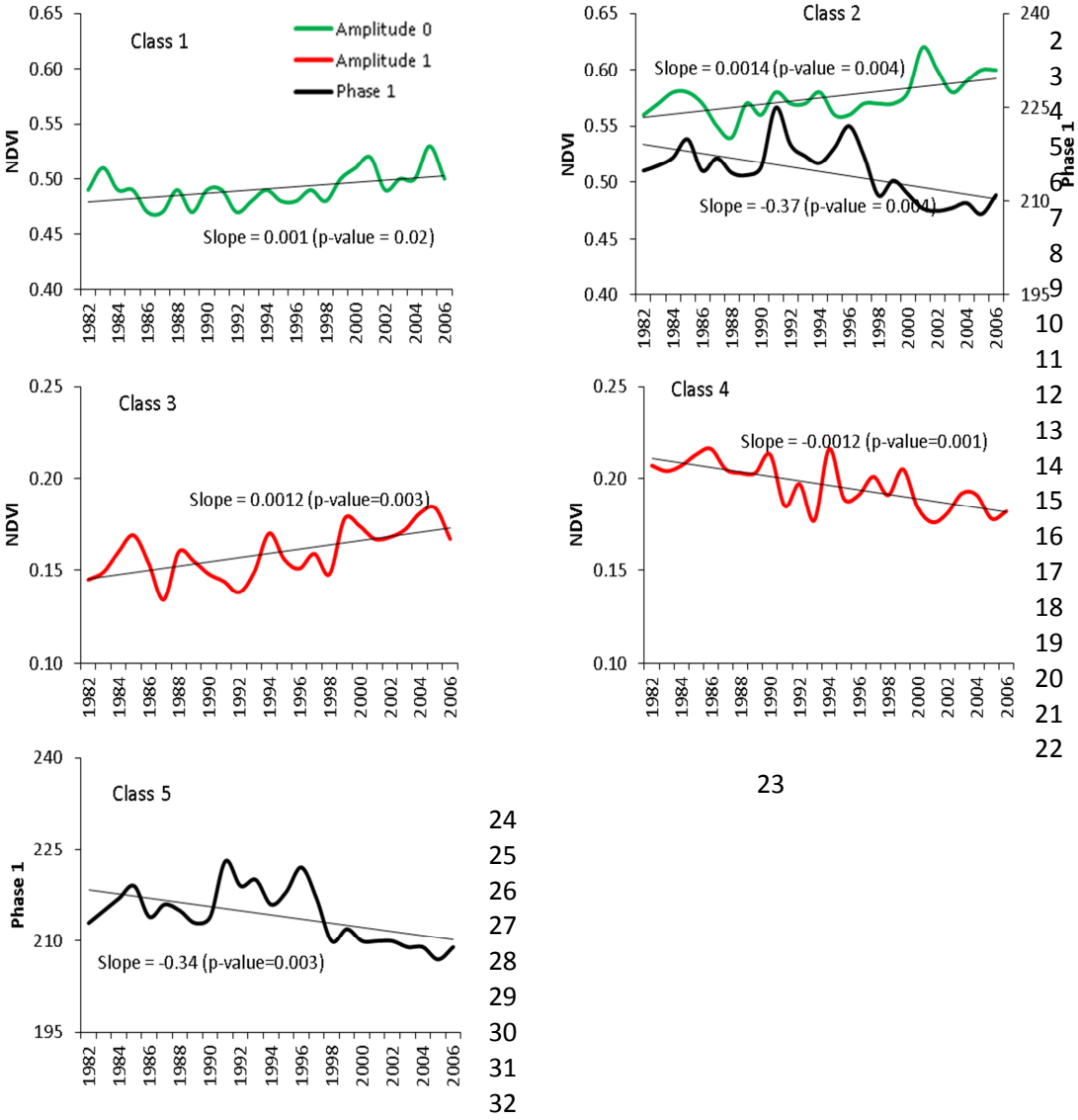

Figure 9. GIMMS-based trends and trend changes on harmonic series shape parameters for: (a) Class 1 (significant increases in Amplitude 0 (Mean NDVI)); (b) Class 2 (significant increases in Amplitude 0 and decrease in Phase 1 (the timing of annual peak greenness) together); (c) Class 3 (significant increases in Amplitude 1); (d) Class 4 (significant decreases in Amplitude 1); and (e) Class 5 (significant decreases in Phase 1). No breakpoints are detected in all classes based on the ordinary least squares (OLS) residuals-based MOving SUM (MOSUM) test in BFAST.

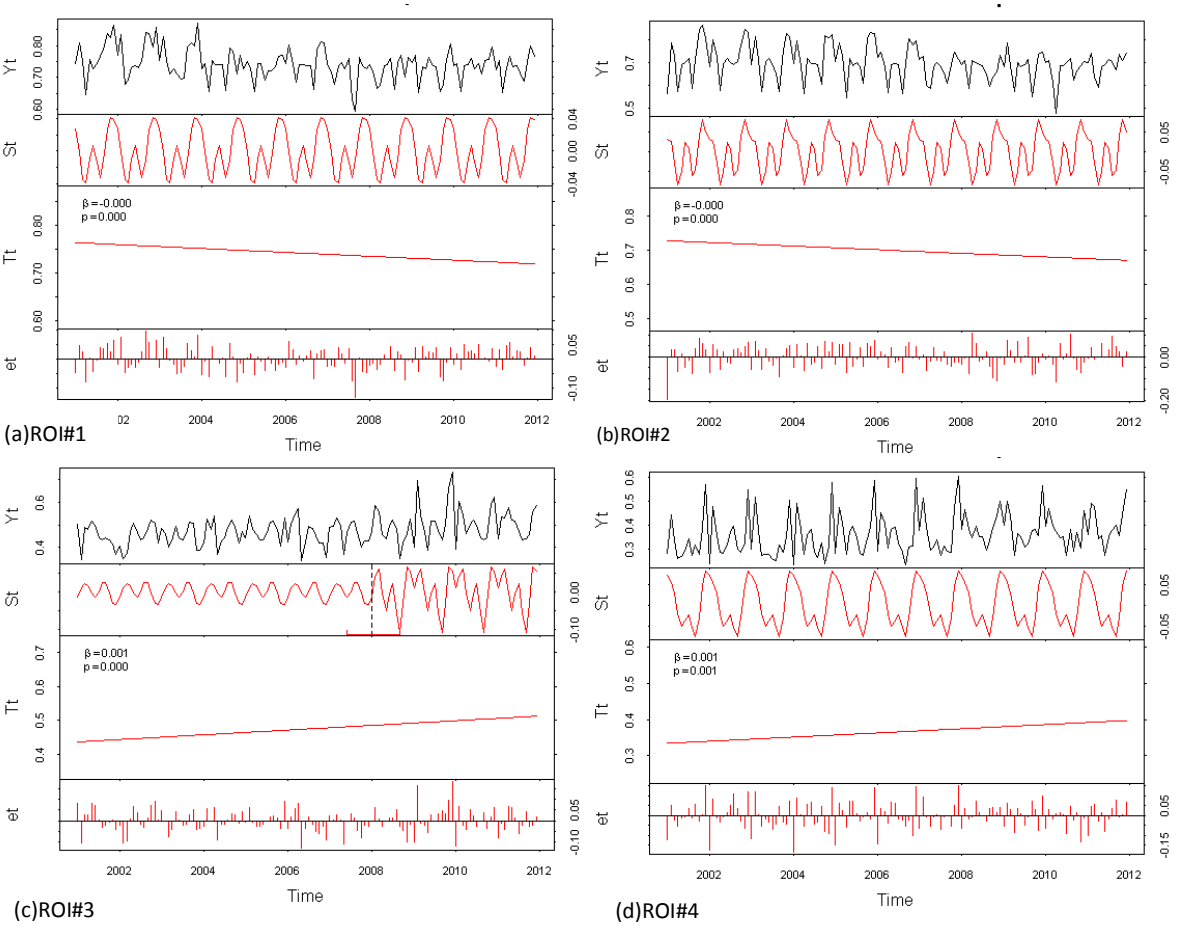

Figure 10. Examples of decomposition and trend break analysis of monthly MODIS NDVI time series (2001-2011) for certain region of interests (ROIs) for significant decreasing trends: (a) ROI #1 and (b) ROI #2 and for significant increasing trends: (c) ROI #3 and (d) ROI #4 generated by BFAST approach. The locations of ROIs are shown in Fig. 3 (d). The top panel in every plot shows the NDVI data, whereas the other three panels depict the individual components after decomposition. The seasonal (S_t) and remainder (e_t) components have zero mean while the trend component (T_t) shows the trend in NDVI. The slope coefficients (β) and the significance levels (P) at α value of 0.05 for each segment are given.

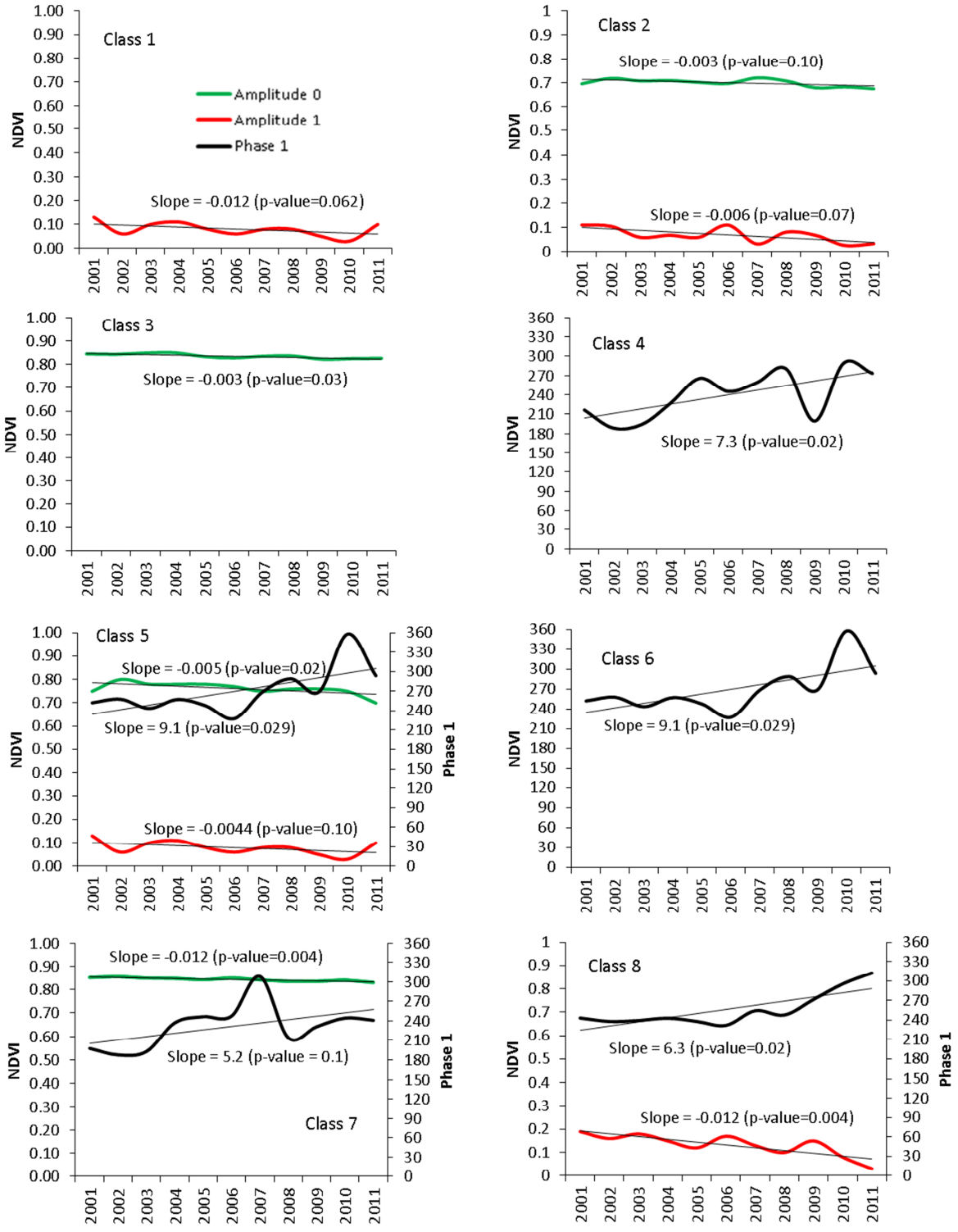

1 Figure 11. MODIS-based trends and trend changes on harmonic series shape parameters for most
2 prevalent classes of significant seasonal trends. The sampled locations are displayed in Figure 8.